Quaternary Science Reviews 303 (2023) 107968

Contents lists available at ScienceDirect

Quaternary Science Reviews

journal homepage: www.elsevier.com/locate/quascirev

Recent global warming induces the coupling of dissimilar long-term sedimentary signatures in two adjacent volcanic lakes (Azores Archipelago, Portugal)

David Vázquez-Loureiro [a], Alberto Sáez [b], Vítor Gonçalves [c, d], Teresa Buchaca [e], Armand Hernández [a], Pedro M. Raposeiro [c], Erik J. de Boer [b, f], Pere Masqué [g, h, i], Santiago Giralt [j], Roberto Bao [a, *]

[a] Universidade da Coruña, GRICA Group, Centro Interdisciplinar de Química e Bioloxía (CICA), Rúa As Carballeiras, 15071, A Coruña, Spain
[b] Department of Earth and Ocean Dynamics, UB-Geomodels Research Institute, Universitat de Barcelona, Martí I Franquès s/n, 08028, Barcelona, Spain
[c] CIBIO, InBIO Laboratório Associado, Centro de Investigação Em Biodiversidade e Recursos Genéticos, Pólo Dos Açores, Rua da Mãe de Deus, 9500-321, Ponta Delgada, Portugal
[d] Faculdade de Ciências e Tecnologia, Universidade Dos Açores, Rua da Mãe de Deus, 9500-321, Ponta Delgada, Portugal
[e] Centre D'Estudis Avançats de Blanes (CEAB-CSIC), C/D'accés a La Cala St. Francesc, 14, Blanes, 17300, Girona, Spain
[f] Departamento de Estratigrafía y Paleontología, University of Granada, Avenida de La Fuente Nueva S/N, 18071, Granada, Spain
[g] International Atomic Energy Agency, 98000, Principality of Monaco, Monaco
[h] Institute of Environmental Science and Technology and Physics Department, Universitat Autonoma de Barcelona, Bellaterra, 08193, Spain
[i] School of Natural Sciences, Centre for Marine Ecosystems Research, Edith Cowan University, Joondalup, WA 6027, Australia
[j] Geosciences Barcelona (Geo3BCN-CSIC), Lluís Solé I Sabarís S/n, 08028, Barcelona, Spain

ARTICLE INFO

Article history:
Received 24 September 2022
Received in revised form
16 January 2023
Accepted 17 January 2023
Available online xxx

Handling Editor: P Rioual

Keywords:
Paleolimnology
Diatoms
Fossil pigments
Global warming
Holocene climate
Remote islands

ABSTRACT

Paleoclimatological information derived from the study of lacustrine sedimentary records is not only biased by taphonomical processes but also by potential differences in the expression of climate variability in the sediments due to site-specific factors. Using a multiproxy approach (the elemental and isotopic compositions of organic matter, diatom assemblages, and marker pigments of algae and cyanobacteria), we study the different environmental signatures recorded since the Little Ice Age (LIA) in the sediments of two volcanic lakes located within the same caldera on São Miguel Island (Azores Archipelago). Lake Santiago is a crater lake whose eutrophic status in the last stage of the LIA was linked to external nutrient inputs associated with this humid period. Its post-LIA evolution was forced by changes in the thermal structure of the water, which determined its degree of mixing and therefore nutrient availability through recycling from the hypolimnion. In contrast, the decadal to centennial limnological evolution of Lake Azul, a caldera lake 2.5 km from Lake Santiago, shows geochemical and micropaleontological signatures disconnected from climate variability until 1980/1990 CE due to its greater exposure to the fallout of tephra after a catastrophic eruption in c. 1290 CE. Only after 1980/1990 CE did a global warming scenario induce a common ecological restructuring of both lakes, involving the replacement of turbulence-loving algal taxa by species adapted to strengthening water column stratification. Nevertheless, this shift was relatively gradual in Lake Azul but more sudden in Lake Santiago, indicating that the local site-specific components still had an effect on the expression of climate change in the sediments. Despite the short history of anthropogenic pressure (compared to their continental counterparts) and the large atmospheric patterns operating over the Azores Archipelago, the sedimentary records of these two adjacent oceanic volcanic lakes reacted quite differently to climate changes.

* Corresponding author. Universidade da Coruña, GRICA Group, Centro Interdisciplinar de Química e Bioloxía (CICA), Rúa As Carballeiras, 15071, A Coruña, Spain.
E-mail addresses: david.vazquez@udc.es (D. Vázquez-Loureiro), a.saez@ub.edu (A. Sáez), vitor.mc.goncalves@uac.pt (V. Gonçalves), buch@ceab.csic.es (T. Buchaca), armand.hernandez@udc.es (A. Hernández), pedro.mv.raposeiro@uac.pt (P.M. Raposeiro), deboer.erikjan@gmail.com (E.J. de Boer), p.masque@ecu.edu.au (P. Masqué), sgiralt@geo3bcn.csic.es (S. Giralt), roberto.bao@udc.es (R. Bao).

https://doi.org/10.1016/j.quascirev.2023.107968

1. Introduction

Natural and human-induced impacts on ecosystems are characterized by large spatial and temporal variability in their nature, duration, and intensity (Jackson and Hobbs, 2009). When studying processes operating at temporal scales that are much larger than those typically addressed by neoecologists, paleoecological studies are highly relevant (Louys, 2012). With its decadal to millennial perspective, paleoecology provides a unique understanding of how ecosystem services can be preserved over time, as well as information on baseline environmental contexts and ecosystem alternative stable states (Jeffers et al., 2015).

However, the reliability of paleoecological archives depends on several factors. Taphonomical processes, such as selective preservation, postmortem transport, time averaging or diagenetic effects, are known to bias the information provided by the fossil record (e.g., Raposeiro et al., 2018; Saraswati and Srinivasan, 2015). It is less known how the signatures of the environmental drivers recorded in the sedimentary archive are influenced by site-specific differences, despite being essential for addressing the effects of recent climate change (Hargan et al., 2016; Seddon et al., 2014).

Lakes act as excellent sentinels of environmental change (Williamson et al., 2008, 2009), but they integrate local and global signals into sedimentary records previously modulated by the atmosphere and lake catchments (Leavitt et al., 2009; Ritter et al., 2022). Site-specific variability affecting soil type, vegetation, topography, or basin morphometry, among others (Jovanelly and Fritz, 2011), is already known to account for many of the differences in the expression of environmental drivers of change in lacustrine sedimentary records (Hargan et al., 2016; Rühland et al., 2015). This expression can also differ in a single lake throughout its development, resulting in a lack of linear responses of the sediment records to climate forcing (Bao et al., 2015; Hernández et al., 2008). Therefore, fundamental questions arise about the possibility of disentangling climate vs. nonclimate forcings when analyzing lake sediments (Mills et al., 2017).

The sedimentary records of temperate low-elevation lakes on oceanic islands can potentially better preserve climatic information than their continental counterparts, since the human occupation of such areas often occurred in recent historical times and usually began with low population densities (Keegan and Diamond, 1987; Nogué et al., 2021), resulting in much shorter time spans of human disturbances. In addition, the climate of oceanic islands is usually controlled by large atmospheric and oceanic patterns and is less impacted by the continental effects of local convection (Sáez et al., 2009). Both conditions, namely, only recent anthropogenic pressures and large atmospheric and oceanic patterns governing climate, are present in the Azores Archipelago, located in the middle of the Atlantic Ocean (Fig. 1). On the one hand, the colonization of the Azores extends back to just ca. 700–850 CE, although it was not until ca. 1070–1280 CE that human presence became more prominent on the landscape (Raposeiro et al., 2021; Richter et al., 2022). On the other hand, the climate conditions of the archipelago are mostly controlled by the North Atlantic Oscillation (NAO), the main large-scale climate mode of variability in this region (Hernández et al., 2016, 2020). A previous comparison of instrumental and proxy-based reconstructions for the pre-instrumental period showed that climate was the main control in the long-term sedimentary dynamics of Lake Empadadas (Hernández et al., 2017), a shallow volcanic lake located on the west side of São Miguel Island (Fig. 1). In contrast, Lake Azul, a deep lake within a volcanic caldera (Caldeira das Sete Cidades), was exposed to a massive influx of tephra after an eruptive event in ca. 1290 CE (Raposeiro et al., 2017) (Fig. 1) and has experienced a long-term ecological trajectory mainly determined by the oligotrophic inertia forced by this natural catastrophic episode (Vázquez-Loureiro et al., 2019). An intersite comparison of lake paleorecords should therefore show either a good correspondence of signals, thereby reflecting regional-scale climatic and environmental change, or a poor fit resulting from site-specific local components or 'noise' (Roberts et al., 2016).

Thus, we can hypothesize that large differences in the sensitivity of volcanic lakes to climate variability should be attenuated when the lakes are separated by short distances and fall within the same volcanic center. Here, we present the paleoecological evolution of Lake Santiago, a deep volcanic lake located in the Caldeira das Sete Cidades on São Miguel Island (Fig. 1), and compare it to that of Lake Azul, which is located in the same volcanic center, just 2.5 km from Lake Santiago. We use instrumental climate data, as well as the independent paleoclimate record of Lake Empadadas (Hernández et al., 2017), located 5.0 km outside of the Caldeira das Sete Cidades, to determine the major climate phases of the archipelago since 1350 CE and how the two deep lakes, Lake Santiago and Lake Azul, have responded to climate changes.

2. Study site

The Azores Archipelago comprises nine main islands of volcanic origin that have developed at the triple junction of the American, African and Eurasian tectonic plates (Andrade et al., 2021) (Fig. 1A). The caldera of Sete Cidades represents an active volcanic center located on the western part of the island of São Miguel (Fig. 1B) and contains a set of lakes with contrasting morphologies and degrees of volcanic activity. Lake Santiago (37°50′ N, 25°46′ W) is in the southeasternmost part of the caldera, while Lake Azul (37°52′ N, 25°46' W) is in the northernmost part.

The basin of Lake Santiago (Fig. 1D) occupies the bottom of a crater originating from hydromagmatic eruptions (360 m asl) and is surrounded by steep walls composed of pumice rocks. The walls are covered by a woodland dominated by the introduced coniferous tree *Cryptomeria japonica* (Thunb. Ex L. f.) D. Don. The lake has an elliptical shape, with its maximum axis oriented N–S, an area of 0.25 km^2, and maximum and average depths of 32 and 13 m (Fig. 1D), respectively (Pereira et al., 2014). The surface area to catchment ratio in Lake Santiago is 0.23 (Supplementary Table 1). Lake Azul is the largest lake of the Azores, with a surface of 3.59 km^2 and a maximum depth of 28 m (Fig. 1C), and is located inside the caldera (259 m asl) yielding a surface area to catchment ratio of 0.31. The lake basin has two main morphological areas: a shallow platform (0–12 m) and a deep plateau (25–28 m). Both Lake Santiago and Lake Azul exhibit monomictic characteristics, with stratification in the summer period.

The archipelago features an oceanic temperate climate, with mild temperatures, frequent winds, high relative air humidity, and a precipitation regime with a strong seasonal cycle and high interannual variability (Hernández et al., 2016). The position of the semipermanent high-pressure Azores Anticyclone and the Azores Current (a branch of the Gulf Stream) are the main factors driving climate (Volkov and Fu, 2010). The climate variability of the Azores Archipelago is further influenced by large-scale climate modes, such as the NAO, the East Atlantic pattern (EA) and the Atlantic Multidecadal Oscillation (AMO) (Andrade et al., 2008; Hernández et al., 2016, 2017; Yamamoto and Palter, 2016).

3. Material and methods

3.1. Field methods and core lithologies

A total of six sedimentary cores were retrieved from three different locations in Lake Santiago in September 2011 using a

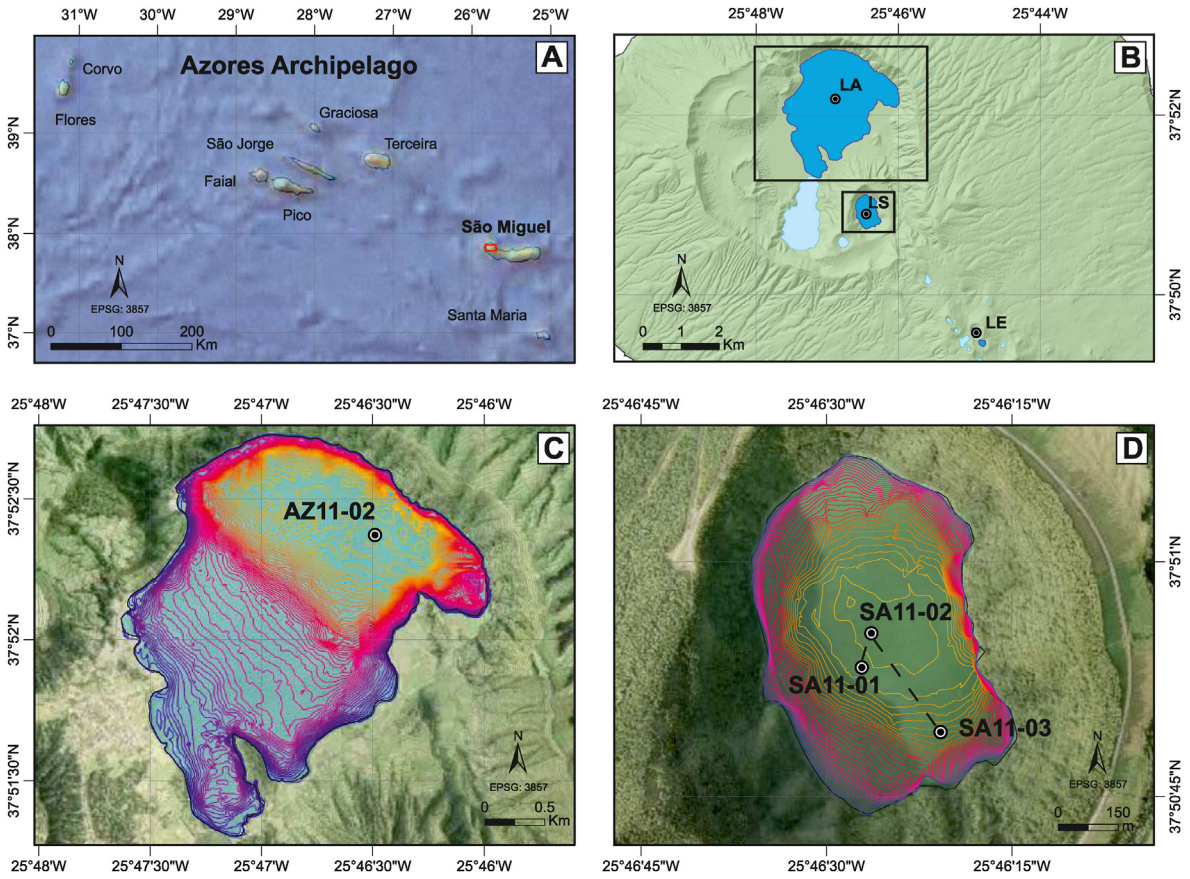

Fig. 1. A. Location of the Azores Archipelago and São Miguel Island. B. Location of the Sete Cidades caldera on São Miguel Island with Lake Santiago (LS), Lake Azul (LA) and Lake Empadadas (LE). C. Bathymetric map of Lake Azul showing the location of core AZ11-02 described in Vázquez-Loureiro et al. (2019). D. Bathymetric map of Lake Santiago showing the location of the recovered cores.

UWITEC© gravity corer (Fig. 1D): (1) offshore cores SA11-01 A and SA11-01 B (Site 1: 37° 50′ 53″ N – 25° 46′ 26″, 27 m), (2) offshore cores SA11-02 A and SA11-02 B (Site 2: 37° 50′ 56″ N – 25° 46′ 27″, 31.5 m) and (3) cores SA11-03 A and SA11-03 B (Site 3: 37° 50′ 49″ N - 25° 46' 21" W, 25.3 m). The description of the sediments includes lithology, texture, color, and structures that allowed the definition of facies and lithostratigraphic units and a correlation among the six cores. A composite sequence (SA11-02) was constructed using cores SA11-02 A and SA11-02 B (Fig. 2), representing sedimentation in a pelagic environment. A multiproxy approach based on diatoms, organic pigments, and the elemental and isotopic compositions of the records provides the basis for paleoenvironmental reconstruction.

3.2. Dating methods

The relative concentrations of ^{210}Pb were determined by high-resolution gamma spectrometry (Appleby, 2001), and a constant flux:constant sedimentation (CF:CS) model was constructed for the top of the SA11-02 column (Supplementary Fig. 1). Accelerator mass-spectrometry (AMS) ^{14}C dating from different cores, calibrated to calendar years (cal yr CE) using the CALIB 7.1 software (Stuiver, 1993), and the INTCAL13 curve (Reimer et al., 2013) were also used for the remaining part of the composite column. Because of variations in the reservoir effect in dissolved inorganic carbon (DIC) due to the contribution of CO_2 of igneous origin (Andrade et al., 2019), only the ^{14}C dates from terrestrial plant macrorest samples were used to construct the age model, disregarding those from bulk organic matter (Supplementary Table 2).

The age model was constructed by linear interpolation between the tie-points resulting from the different dating methods. Additionally, to validate the constructed chronological model, samples were checked for the first appearances of pollen of the exotic Japanese Cedar (*Cryptomeria japonica*) and *Pinus* spp. As their years of introduction on the island are known.

3.3. Pollen analyses

Twelve pollen samples of 0.5 cm^3 were strategically taken along the core. Sample preparation included treatments with KOH, HCl, HF, and acetolysis following standard procedures in unison with other paleoecological studies in the Azores (Raposeiro et al., 2021; Ritter et al., 2022). Slides were investigated for indicative pollen and spore taxa, as well as nonpollen palynomorphs, related to ecological shifts, human impact, erosion, fire and other landscape processes, at × 400 magnification.

3.4. Diatom analyses

Samples for diatom analysis were treated following standardized procedures (Renberg, 1990), and slides were prepared with Naphrax© mountant. At least 400 diatom valves were counted at × 1000 magnification using a Nikon Eclipse 600 microscope with Nomarski differential interference contrast optics. Taxa were identified using standard references (e.g., Krammer, 2000, 2002, 2003; Krammer and Lange-Bertalot, 1986–1992; Lange-Bertalot,

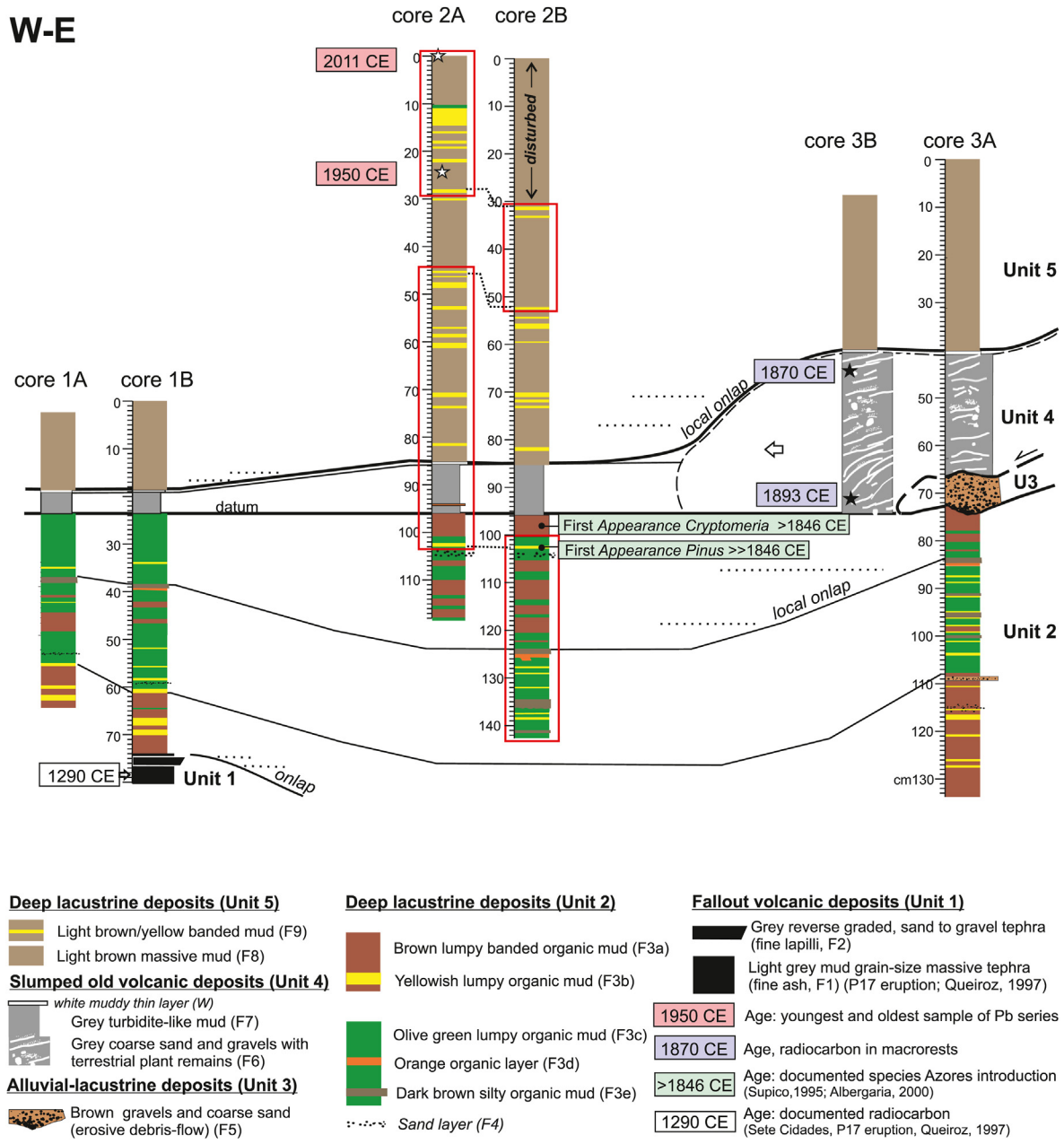

Fig. 2. Stratigraphic correlation panel of the six cores retrieved in Lake Santiago (location of cores indicated in Fig. 1). Sedimentary units, facies, onlap surfaces and age tie-points are represented. The arrow indicates the presumed slump transport of the deformed materials of Unit 4. Red rectangles in cores 2 A and 2 B indicate the stretches used for the construction of the composite column.

2001; Lange-Bertalot et al., 2011; Levkov, 2009; Levkov et al., 2013), and other sources for specific taxa (e.g., Houk and Klee, 2007; Lange-Bertalot and Ulrich, 2014; Potapova et al., 2008). All identifications were revised according to the available information from the Azores Archipelago (Goncalves et al., 2010).

3.5. Pigment analyses

A total of 34 samples were used for pigment analyses, using freeze-dried sediments stored in dark conditions. The pigments were extracted from sediments using 90% acetone with a probe sonicator (Sonopuls GM70 Delft, The Netherlands) (50 W, 2 min). The extract was centrifuged (4 min at 3000 rpm, 4 °C), filtered through Whatman ANODISC 25 (0,1 μm) and analyzed with ultrahigh-performance liquid chromatography (UHPLC) following the method described by Buchaca et al. (2019). Pigments were identified by comparison with a library of pigment spectra obtained from extracts of pure algae cultures from the Culture Collection of Algae and Protozoa (CCAP, Oban, Scotland, UK) and pigment standards (DHI Water and Environment, Hørsholm, Denmark). Pigments with a high taxonomic affinity were selected, including β-carotene (all groups), alloxanthin (cryptophytes), aphanizophyll (N_2-fixing cyanobacteria), canthaxanthin and echinenone (mainly cyanobacteria), diadinoxanthin (mainly dinoflagellates), diatoxanthin (diatoms), zeaxanthin (chlorophytes and cyanobacteria) and lutein (chlorophytes). We also analyzed Chl-*a* and its derivative products, including chlorophyllide a, allomers and epimers of Chl-*a*, phaeophorbide-a and phaeophythins-a and -b. We defined the sum

of Chl-*a* and Chl-*a* derivatives as a-phorbin. We based interpretation on carotenoid profiles instead of phorbins because there is a higher loss of phorbins than of carotenoids to undetectable colourless compounds when pigments are deposited and buried (Buchaca and Catalan, 2008). Furthermore, we calculated a Chl-*a* preservation index as the Chl-*a*:a-phorbin ratio. The index is scaled from 0 (low Chl-*a* preservation) to 1 (high Chl-*a* preservation) (Buchaca and Catalan, 2007). Values for pigment abundances were expressed as μmol g^{-1} TOC. The molecular weights of the different pigments were obtained from Jeffrey et al. (1997).

3.6. Geochemistry methods

A Finningan delta Plus EA–CF–IRMS spectrometer at the Centers Científics i Tecnològics of the Universitat de Barcelona (CCiTUB) was used to determine the total carbon (TC), total nitrogen (TN), and isotopes of carbon ($\delta^{13}C_{org}$) and nitrogen ($\delta^{15}N_{org}$) of bulk organic matter. Since X-ray diffraction analyses did not detect any carbonates, TC equals the total organic carbon (TOC) (Raposeiro et al., 2017). For the discrimination of the inorganically bound nitrogen content from TN, we used the correction by Talbot (2001). The TOC/TN ratio is therefore referred to as TOC/TN_{corr}.

3.7. Statistical methods

Statistical analyses for the diatom data were performed on the square-root transformed relative abundance matrix expressed as percentages. Only taxa that reached >5% in at least one sample were included in the analyses. The software Psimpoll 4.10 (Bennett, 2002) was used to define the main diatom assemblage zones (DAZs) by means of stratigraphically constrained cluster analysis based on squared Euclidean distance (CONISS (Grimm, 1987). Zonations with variances exceeding values generated by a broken-stick model of variance distribution were considered statistically significant (Bennett, 1996). CANOCO 4.5 software (ter Braak and Šmilauer, 1998) was used to perform two ordination techniques, detrended correspondence analysis (DCA) and principal component analysis (PCA). The former was used to measure the length of the primary environmental gradient (Šmilauer and Leps, 2014), and the latter was used to determine the environmental controlling factors in the composition of the diatom assemblages. PCA was also applied to organic pigments on a compositional data matrix, including a selection of eight marker pigments following taxa affinity and preservation criteria. Both PCA and chronological clustering were used to identify potential threshold responses in the data series (Andersen et al., 2009).

4. Results

4.1. Sedimentary facies and units

From the stratigraphic correlation of six cores retrieved from Lake Santiago, we recognized five sedimentary units numbered chronologically from base to top (Fig. 2):

Unit 1. This unit corresponds to volcanic deposits that were retrieved from the lower 6 cm of core 1 B. It is composed of light gray massive tephra (fine ash) fallout deposits, has a muddy grain size, and is barren of lacustrine fauna and flora (Facies F1, Fig. 2). The ash is intercalated with a gravel, reverse graded, pumiceous layer that corresponds to fine lapilli deposits (Facies F2, Fig. 2). Correlation of the cores shows an onlap geometry of Unit 2 deposits covering this volcanic unit, indicating an undulating top geometry (Fig. 2). The stratigraphic position and characteristics of these volcanic deposits (Facies F1) suggest a correspondence with the upper part of the eruptive episode P17 in the Sete Cidades caldera (Queiroz, 1997). This major eruptive episode has been identified in the sedimentary record of Lake Azul and Lake Empadadas and has been dated to ca. 1290 CE (Hernández et al., 2017; Raposeiro et al., 2017).

Unit 2. This unit is recovered in all cores and has a minimum thickness of 50 cm. It is made up of a banded, varicolored lumpy, organic mud and is rich in planktonic diatoms and the remains of other lacustrine organisms (Facies F3, Fig. 2). The colors of this unit are brown (F3a), yellowish (F3b), olive green (F3c), and orange for a single thin bed (F3d). It also shows several dark brown silty layers (F3e) and thin gray sandy horizons (Facies F4, Fig. 2). Considering their characteristics and location in the modern lake, the deposits of Unit 2 accumulated in deep, offshore lacustrine conditions. The top of this unit records the first appearance of pollen from the introduced coniferous trees *Cryptomeria japonica* and *Pinus* spp., indicating that the lower part of the unit was deposited before 1864 CE (De Albergaria, 2000; Supico, 1995).

Unit 3. This unit is recorded in eastern core 3 A and consists of a nonvolcanic, highly erosive, brown, sandy gravel layer up to 60 cm thick. This facies is barren of fossil remains and displays debris flow features. We interpret this unit as the local arrival of a high-energy alluvial flood (Facies F5, Fig. 2). The age of this unit is expected to be close to the age of Unit 4, as both units correspond to the deposit of a single high-energy event.

Unit 4. This unit, recovered in all cores, corresponds to a gray interval up to 75 cm thick overlapping Units 2 and 3. There is a lateral change in facies in this unit. In cores 3 A and 3 B, it is composed of pumice-rich tephra and disorganized sandy gravel material that preserve traces of fallout structures (Facies F6, Fig. 2). This facies shows plastic deformation features, attributed to a slump process that occurred in a pre-existing coarse pyroclastic deposit. These coarse deposits are barren of lacustrine fossils, except for some terrestrial plant remains that must have been incorporated into the mass of coarse material during their transport from slumping. Toward the western cores, these coarse deposits form 10-20 cm-thick distal laminated to massive gray muddy deposits, rich in lacustrine organism remains, deposited by decantation of a cloud of fine suspended particles segregated from the coarse-grain mass slump episode (Facies F7, Fig. 2). A whitish 1 cm-thick horizon (layer W) covers all deposits in this unit (Fig. 2). The age of Unit 4 is constrained between the radiocarbon dates from plant macrorests found at its top and bottom in core SA11-03 B corresponding to 1868 CE and 1893 CE, respectively.

Unit 5. This unit is recovered in all cores, has a maximum thickness of 85 cm and is composed of light brown massive mud (Facies F8, Fig. 2), alternating with intervals of light brown mud with interbedded yellow bands (Facies F9, Fig. 2). These deposits, rich in lacustrine organism remains, accumulated in deep offshore conditions similar to the present ones.

4.2. Age–depth model of the composite core

To construct the age–depth model for the studied composite core, we used a) the lithostratigraphic correlation of the six gravity cores using specific tie-points, b) the ^{210}Pb profile in core SA11-2 A (Supplementary Fig. 1), c) two AMS ^{14}C dates on terrestrial plant macrorests in core SA11-3 B, and d) the known age of the P17 volcanic eruption in core SA11-1 B (Fig. 2), which is the latest large eruption in the Sete Cidades caldera (Cole et al., 2008). The first appearances of pollen grains from the introduced *Cryptomeria japonica* and *Pinus* spp. in core SA11-2 B were used to validate the ages derived from the resulting age model (Supplementary Table 3). The lack of erosive surfaces and onlap geometries in cores SA11-2 A and SA11-2 B used to construct the composite core ensures its sedimentary and temporal continuity.

Based on the CF:CS model of the ^{210}Pb profile, the sedimentation rate for the first 60 yr is 0.42 ± 0.02 cm yr^{-1} (Supplementary Fig. 1). The chronology of this interval covers the uppermost 25 cm. Ages for the top of the composite core (Unit 5) were then estimated by linear interpolation from the topmost sample (dated to 2011 CE, the year of the field sampling campaign) and the base of the ^{210}Pb profile (dated to 1950 CE), as well as from this level to the age at the top of Unit 4 (Fig. 3). The nature of the coarse-grained Units 3 and 4 matches those of the 1870 CE flood event deposits recorded in the adjacent Lake Azul (Vázquez-Loureiro et al., 2019), suggesting that the same high-energy event generated both deposits and, thus, they are of equal age. The sediments of Unit 2 were also dated by linear interpolation between the given age of deposition of Unit 4 (1870 CE) and the known age of the P17 tephra deposit in core SA11-01 B (Unit 1). This deposit corresponds to the most significant and recent eruption (P17, dated to ca. 1290 CE) that deposited tephra in the lakes of the Sete Cidades complex (Queiroz et al., 2008; Shotton and Williams, 1971). The orange organic layer corresponding to Facies F3d was used as a tie-point to correlate cores SA11-01 A, SA11-01 B, SA11-02 B and SA11-03 A (Fig. 2). An additional tie-point, reflected by the sharp change between the brown lumpy and yellowish organic muds (Facies F3a and F3b) and the olive green and dark brown organic muds intercalating the orange organic layer (Facies F3c, e and d, respectively), also allowed correlation among cores SA11-01 A, SA11-01 B, and SA11-03 A. As the lowermost 20 cm of core SA11-02 B (Unit 2) could not be correlated with the rest of the cores, ages were extrapolated by extending the sedimentation rate to this short stretch of the core (Fig. 3).

The first recorded appearances of pollen from *Cryptomeria japonica* and *Pinus* spp. (Fig. 2) almost exactly fit with a) the known introduction of *Cryptomeria japonica* to São Miguel Island dated to 1850-55 CE (De Albergaria, 2000; Supico, 1995) and b) the first noticeable plantations of *Pinus* on the island dated to 1820–1830 CE, after the unsuccessful introduction of the taxon in 1750 CE (Supico, 1995). This finding is also consistent with the first appearance of this pollen in the sedimentary record of the adjacent Lake Azul, also dated to 1820 CE (Rull et al., 2017; Vázquez-Loureiro et al., 2019).

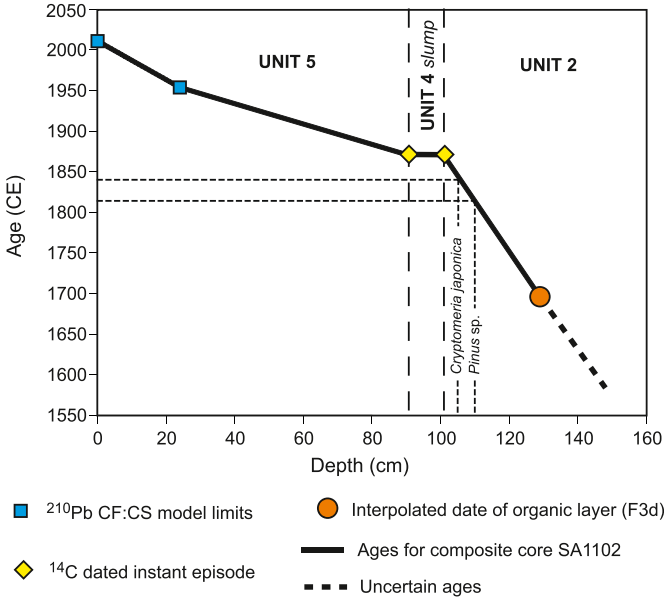

Fig. 3. Age–depth model based on the ^{210}Pb activity–depth profile and the AMS ^{14}C dates. The expected age was calculated using linear interpolation and compared with documentary accounts of the introduction of the nonnative *Cryptomeria japonica* and expansion of *Pinus* spp. (De Albergaria, 2000; Supico, 1995). Corresponding sedimentary units are indicated.

4.3. Diatom assemblages

The diatom record comprises 81 taxa and is dominated by species of the genus *Aulacoseira*, which constitute quasi-monospecific assemblages during several intervals (maximum percent abundance up to 89%) (Fig. 4). These dominant taxa become secondary in the uppermost 8 cm of the composite core, where the assemblages are dominated by *Asterionella formosa* and, to a lesser extent, *Fragilaria crotonensis* and *Fragilaria* cf. *tenera* (Fig. 4). The results of the broken-stick model of the distribution of variance define six DAZs (SAN-01 to SAN-06) based on CONISS (Supplementary Table 4). The longest gradient length of taxa scores resulting from the DCA is 1.94 SD units, indicating that ordination methods based on linear response models, such as PCA, are more appropriate for further interpreting the underlying environmental variables explaining the structure of the diatom assemblages (Šmilauer and Leps, 2014). The first two axes of the PCA explain 65.1% of the total variance (Fig. 5A). *Aulacoseira ambigua* shows the highest score for the first main axis of variation ($PC1_d$, 42.9% of the variance). Other *Aulacoseira* spp. and *Fragilaria gracilis* show high scores, whereas the periphytic *Achnanthidium minutissimum* and *Pseudostaurosira brevistriata* show minimum scores. The second axis of variation ($PC2_d$, 22.2% of the variance) shows the highest scores for *F. crotonensis*, *A. formosa* and *F.* cf. *tenera*. Downcore variations in the first two principal components are plotted in the diatom percent abundance diagram (Fig. 4).

4.4. Marker pigments of algae and cyanobacteria

A total of 20 pigments were identified, including chlorophylls, chlorophyll degradation products and marker carotenoids. We selected pigments to be included in the paleoenvironmental reconstruction following two main criteria: pigment specificity to a taxonomic group or a process (e.g., grazing, diagenesis) and low lability, allowing the signal to persist in the sedimentary record (Supplementary Table 5).

We explored the importance of in-lake planktonic and benthic primary production compared with other carbon sources derived from autochthonous and allochthonous matter and detritus, with the concentration of β-carotene (μmol β-carotene g^{-1} TOC) (Fig. 6). The value along the sediment record can be used as a surrogate for the biomass of in-lake primary producers. The value is slightly higher in some levels of Unit 2, indicating a higher pigmentation in the organic matter deposited. There is a decrease at the top of Unit 2 with a minimum in Unit 4. The organic matter pigmentation increases again at the bottom of Unit 5, with minor changes recorded along this unit. All these results suggest a slightly higher biomass of in-lake primary producers during the deposition of Unit 2.

The dominant pigment throughout the entire record is diatoxanthin, representing diatoms (Bacillariophyta) (Fig. 6). Low values of up to a maximum of 6.4 μmol g^{-1} TOC are recorded in Unit 2, whereas the sediments of Unit 5 show a net increasing trend toward a maximum value of 17.4 μmol g^{-1} TOC, followed by a decrease at the top of the sequence.

The marker pigments of cyanobacteria, especially zeaxanthin, aphanizophyll (indicative of N_2-fixing cyanobacteria) and echinenone and canthaxanthin, are mainly present in Unit 2. Cyanobacteria are also represented in Unit 5, mostly by echinenone at the bottom of DAZ SAN-05.

Lutein, representing chlorophytes, is abundant in both Unit 2 and the bottom half of Unit 5, sharply declining thereafter. The chlorophyte pattern revealed by lutein is confirmed by the

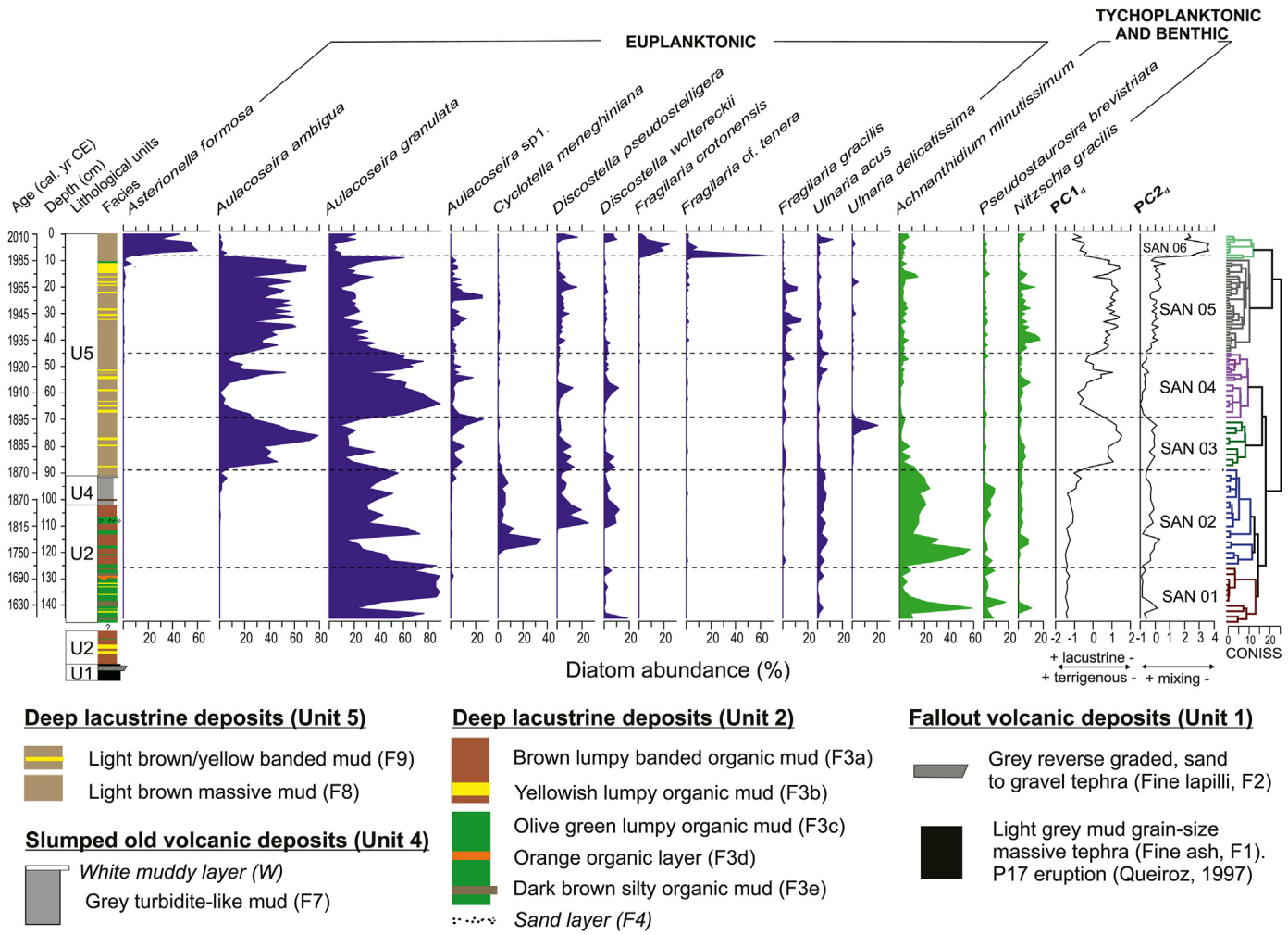

Fig. 4. Diatom percentage abundance diagram for selected taxa (≥5% abundance in at least one sample) in Lake Santiago. The composite column on the left is based on the correlation of offshore cores SA11-02 A and SA11-02 B (see text). Diatoms are grouped according to their habitat preferences. The diatom assemblage zones (DAZs) generated by a broken-stick model of the distribution of variance (Bennett, 1996) are represented by discontinuous lines. The main lithological units and sedimentary facies are also shown. All data are plotted against age (cal yr CE).

pheophytin-b curve, a degradation product of chlorophyll-b, a characteristic pigment of chlorophytes (Supplementary Fig. 2). The topmost sample of the record shows a remarkable peak in alloxanthin, representative of cryptophytes, and a peak in diadinoxanthin, representative of dinoflagellates.

A PCA of pigment composition data reveals two major axes of variation, which explain 76.6% of the variance (Fig. 5B). The first axis ($PC1_p$; 62.0% of the variance) shows a strong positive relation with a diatom marker pigment (diatoxanthin) and a negative correlation with the pigments of the other groups. The second axis ($PC2_p$; 14.5% of the variance) is negatively related to the marker pigments of dinoflagellates (diadinoxanthin), mainly characteristic of cyanobacteria (zeaxanthin, aphanizophyll, canthaxanthin, and echinenone), and that of cryptophytes (alloxanthin), whereas it is positively correlated with the marker pigment of chlorophytes (lutein).

4.5. Organic matter geochemistry

The record shows TOC and TN percent values ranging from 2.51 to 10.54% and 0.29–1.03%, respectively, except for the coarse, volcanic and reworked materials of Unit 4, which show values very close to 0% for both parameters (Fig. 7). Unit 2 exhibits high oscillations in the range of 2.51–10.16% for TOC and 0.29–0.87% for TN. In Unit 5, both TOC and TN show a net increase and stabilization, with values ranging from 4.05 to 10.54% for TOC and 0.53–1.03% for TN (Fig. 7).

The TOC/TN_{corr} profile shows values between 10.58 and 17.25 for Unit 2, with an average value of 13.78. The values in Unit 5 oscillate between 10.98 and 14.57, averaging 12.28.

The $\delta^{13}C_{org}$ curve exhibits values ranging from −25.92 to −20.18‰ in Unit 2 (Fig. 7). Unit 5 shows a peak value of −19.24‰, exhibiting a progressive net decrease thereafter until a minimum of −32.04‰ is reached at the top of the sequence. The $\delta^{15}N_{org}$ curve shows minimum and maximum values throughout the sequence of −2.63 and 2.55‰, respectively. The deposits overlying the tephra, corresponding to Unit 5, show a net increasing trend, with a marked positive excursion occurring in the first 8 cm (Fig. 7).

4.6. Summary of proxy data from Lake Azul

The main proxy data trends from Lake Azul are shown in Fig. 8, and the full results are explained in detail by Vázquez-Loureiro et al. (2019). The record, extending back to the P17 eruptive episode of 1290 CE, shows a net increasing trend in TOC towards the top of the record, with values ranging from 0.18 to 3.53,

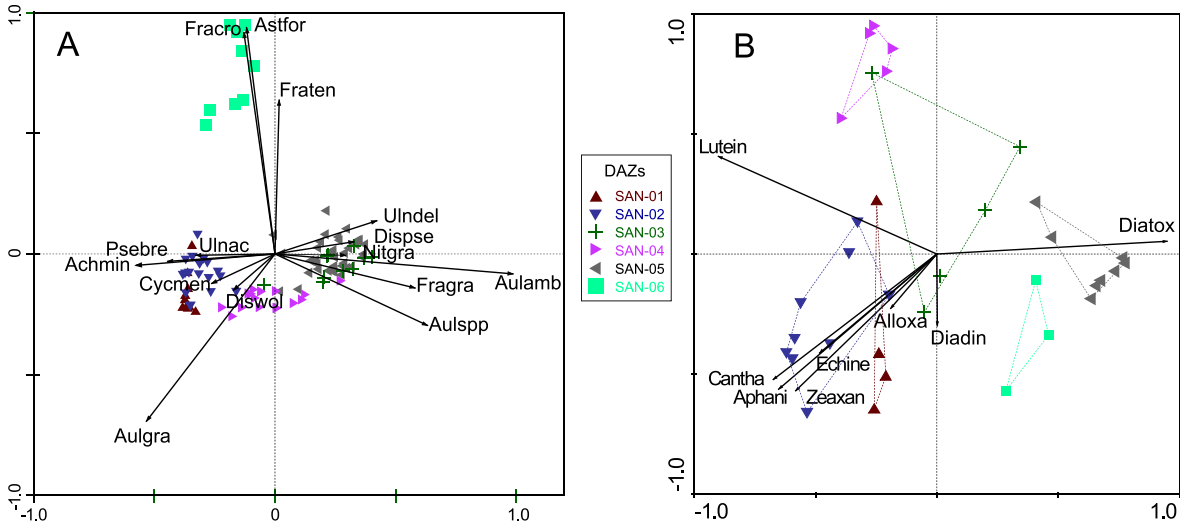

Fig. 5. Principal component analysis (PCA) ordination biplots of samples (numbers) and diatom taxa and pigments in Lake Santiago. Symbols indicate diatom assemblage zones (DAZs) defined by the stratigraphically constrained cluster analysis (see text). A) PCA of the diatom data matrix: Achmin = *Achnanthidium minutissimum*, Astfor = *Asterionella formosa*, Aulamb = *Aulacoseira ambigua*, Aulgra = *Aulacoseira granulata*, Aulspp = *Aulacoseira* spp., Cycmen = *Cyclotella meneghiniana*, Dispse = *Discostella pseudostelligera*, Diswol = *Discostella woltereckii*, Fracro = *Fragilaria crotonensis*, Fragra = *Fragilaria gracilis*, Fraten = *Fragilaria tenera*, Nitgra = *Nitzschia gracilis*, Psebre = *Pseudostaurosira brevistriata*, Ulnacu = *Ulnaria acus*, Ulndel = *Ulnaria delicatissima*. B) PCA of the marker pigment composition data matrix: Alloxa = alloxanthin (cryptophytes), Aphani = aphanizophyll (N_2-fixing cyanobacteria), Cantha = canthaxanthin and Echine = echinenone (mainly cyanobacteria), Diadin = diadinoxanthin (mainly dinoflagellates), Diatox = diatoxanthin (diatoms), Zeaxan = zeaxanthin (mainly cyanobacteria) and Lutein (chlorophytes).

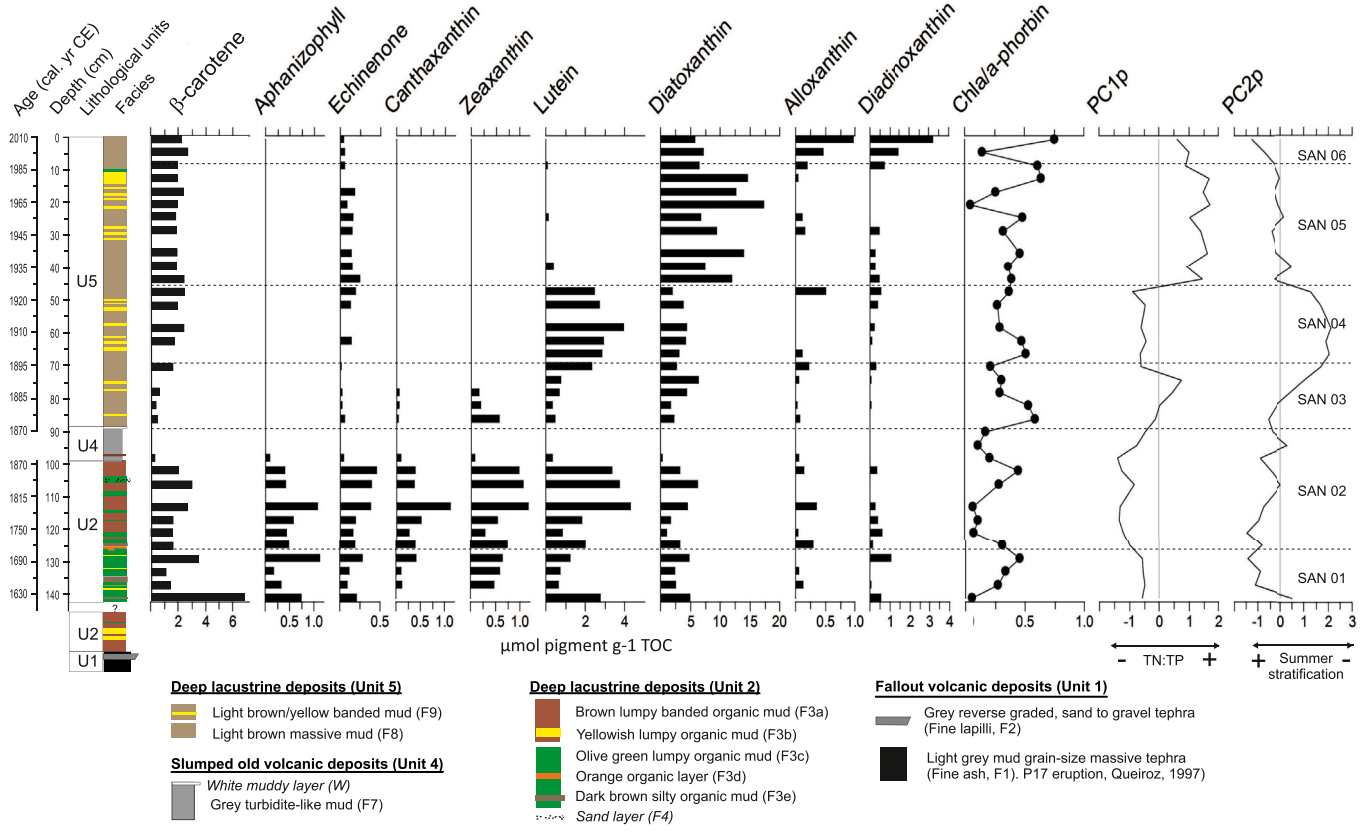

Fig. 6. Pigment diagram (marker pigments) for Lake Santiago. The composite column on the left is based on the correlation of offshore cores SA11-02 A and SA11-02 B (see text). Discontinuous lines represent diatom assemblage zones (DAZs). The main lithological units and sedimentary facies are also shown. All data are plotted against age (cal yr CE). All marker pigments are expressed as µmol g^{-1} TOC. A Chl-*a* preservation index was calculated and plotted as the Chl-*a*:a-phorbin ratio, and the index is scaled from 0 (low Chl-*a* preservation) to 1 (high Chl-*a* preservation).

whereas a progressive reduction in the TOC/TN_{corr} values occurs since c.1600 CE to the present. The diatom assemblages show an almost continuous record of *A. granulata* from c. 1870 to 1980 CE, with a maximum value of 28.2% at c. 1940 CE. The most striking

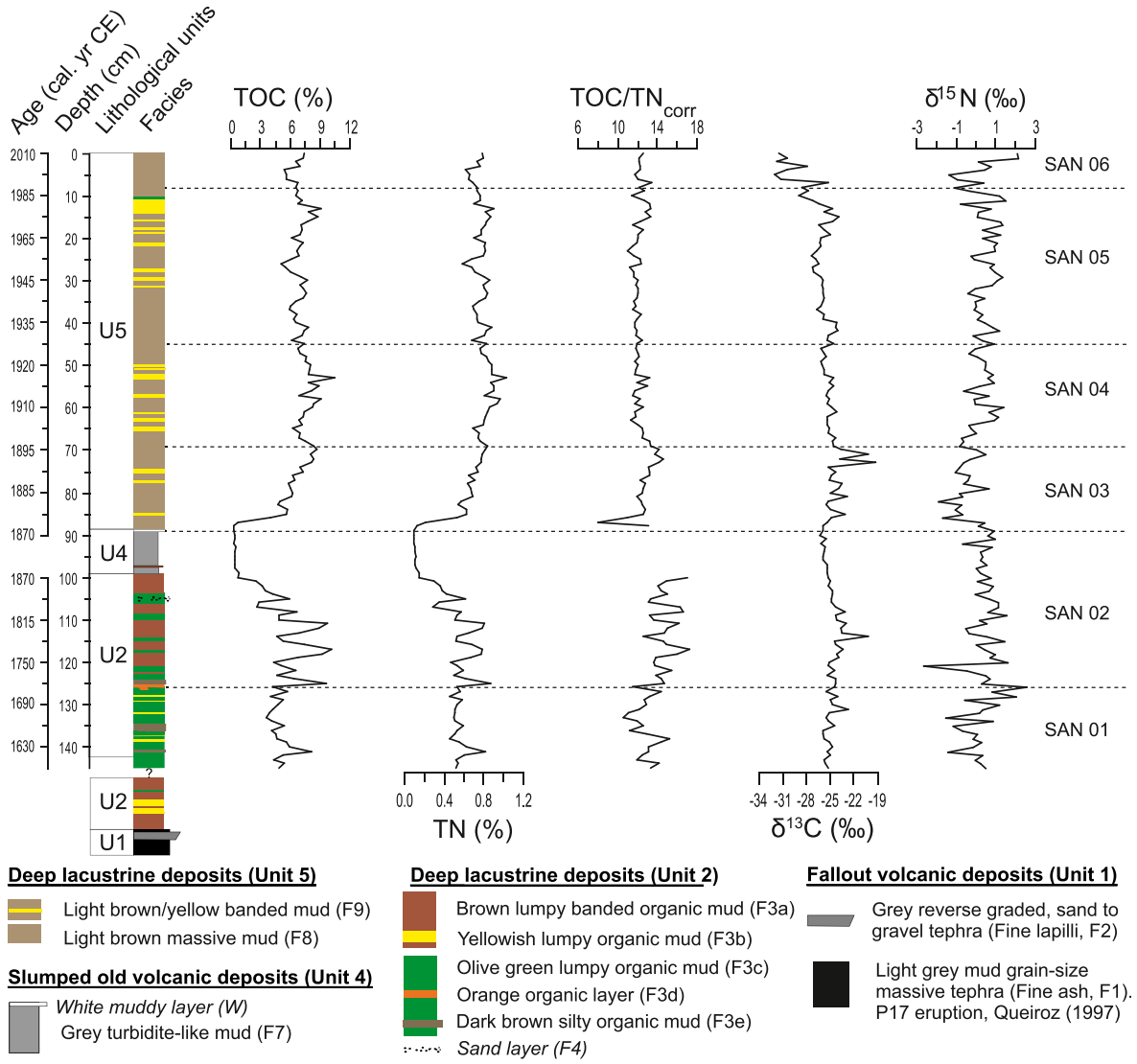

Fig. 7. Geochemical proxy data for Lake Santiago. Proxies include percent total organic carbon (%TOC), percent total nitrogen (%TN), TOC/TN_{corr} ratio (following Talbot (2001)), and carbon and nitrogen isotopes of organic matter ($\delta^{13}Corg$, $\delta^{15}Norg$). The composite column on the left is based on the correlation of offshore cores SA11-02 A and SA11-02 B (see text). Diatom assemblage zones (DAZs) are represented by discontinuous lines. The main lithological units and sedimentary facies are also shown. All data are plotted against age (cal yr CE).

feature at the top of the record is the dominance or codominance of an assemblage made up by *A. formosa*, *F.* cf. *tenera*, and *F. crotonensis*.

5. Discussion

5.1. Drivers of algal assemblage composition in Lake Santiago

The ordination analyses of the main marker pigment composition (PCA_p) and diatom species percent abundance data (PCA_d), along with the geochemical data, explain the main environmental factors controlling the long-term composition of primary producers in Lake Santiago.

The most abundant diatom species throughout most of the core sequence, the eutrophic *Aulacoseira granulata*, shows high absolute scores for the first two components of the PCA_p ($PC1_d$ and $PC2_d$), indicating that both environmental gradients decisively affect the abundance of this species in the record (Fig. 5A). The mesotrophic euplanktonic *Aulacoseira ambigua* and *Aulacoseira* spp. show the highest positive correlation for $PC1_d$, whereas two periphytic taxa, *Achnanthidium minutissimum* and *Pseudostaurosira brevistriata*, show the highest negative scores for this axis. Additionally, the more terrigenous features of Unit 2 vs. Unit 5, as well as the recorded highest values of the TOC/TN_{corr} ratio in the former, indicate enhanced inwash from the catchment (Meyers and Teranes, 2001) and, therefore, lateral advection of periphytic diatoms from the littoral areas to this deep/inner position of the lake (e.g., Bao et al., 1999). We therefore interpret this component as a reflection of the relative importance of lacustrine vs. terrigenous sedimentation.

Asterionella formosa, *F. crotonensis*, and *F.* cf. *tenera* are positively correlated with $PC2_d$, whereas *A. granulata* is negatively correlated. The two opposing groups of diatoms show specific adaptations to thrive under different turbulence regimes. *Asterionella formosa*, *F. crotonensis*, and *F. tenera* show buoyance capabilities, making them more competitive under more stable water column conditions, whereas the heavily silicified *Aulacoseira* requires well-mixed waters (Rühland et al., 2015). We therefore interpret this axis to be

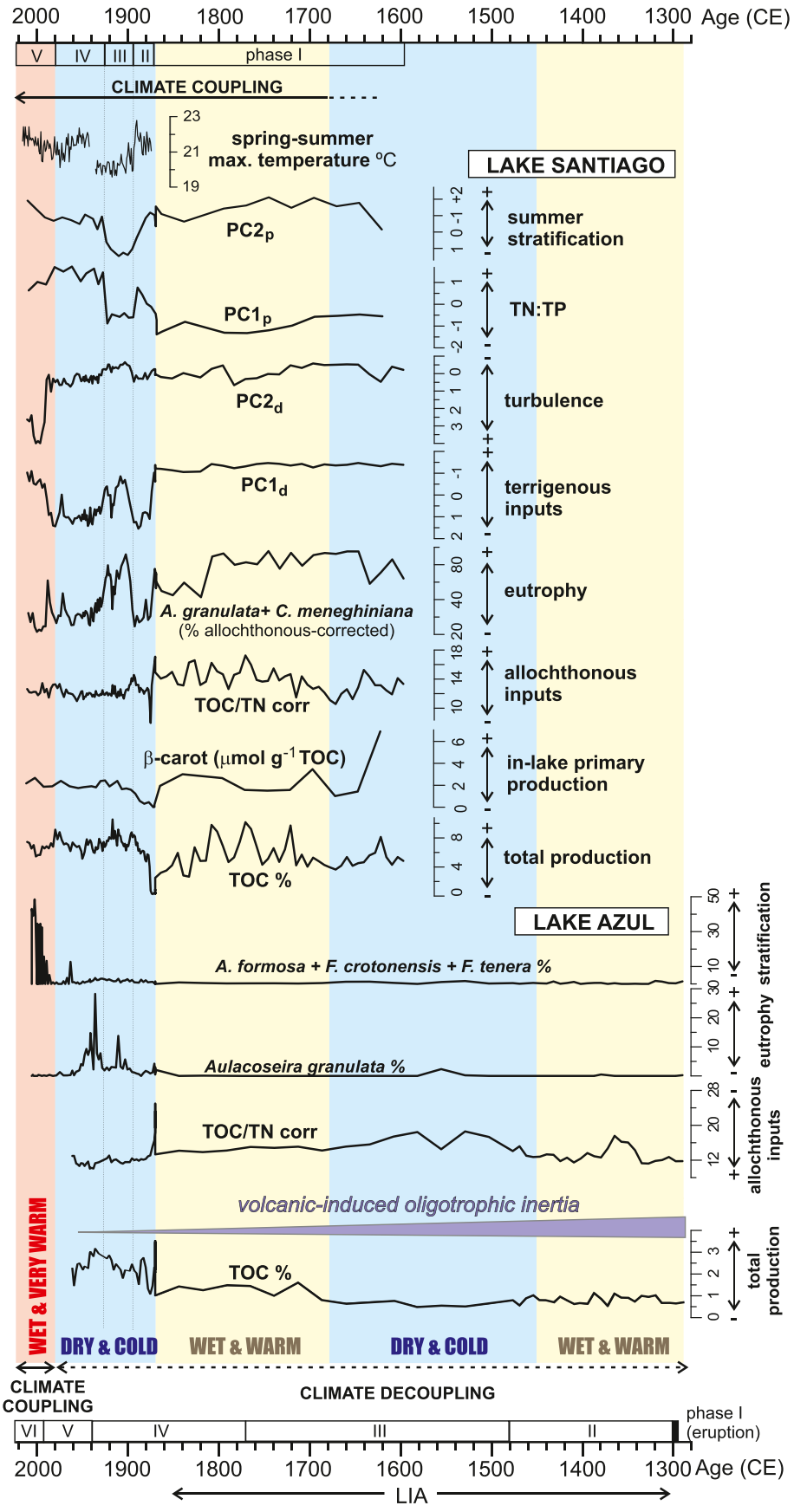

Fig. 8. Comparison of the main environmental patterns of change in Lake Santiago and Lake Azul under the climate stages defined by Hernández et al. (2017) for the archipelago and the instrumental spring and summer (MAMJJA) maximum air temperature (MAT) record of Ponta Delgada (Cropper and Hanna, 2014). Data from Lake Azul are derived from

related to the frequency and/or duration of the lake mixing period and thermal stratification strength.

The PCA_p results of the pigment compositional data reveal that the major axis of variation ($PC1_p$) is positively related to diatoms and negatively related to chlorophytes, cyanobacteria, and cryptophytes (Fig. 5B). Following resource competition theory, chlorophytes and cyanobacteria are better competitors for N and light than diatoms and therefore dominate at low N:P and light:P ratios (Tilman et al., 1986). The allocation at different ends along this axis of algal groups showing distinct element uptake ratios suggests that this axis is related to changes in the N:P stoichiometry of the water column. The second major axis of pigment compositional variation ($PC2_p$) is positively related to chlorophytes and negatively related to dinoflagellates, cyanobacteria, and cryptophytes. Diatoms, characteristic of the spring early stage of phytoplankton succession in lakes, barely contribute to this axis (Fig. 5B), suggesting that this component accounts for only the late-spring to summer lake conditions, when silica depletion and thermal stratification favor the algal groups located along this axis (Margalef, 1983). The algal group positively correlated with $PC2_p$ is the chlorophytes, a group with a high contribution of nonmotile taxa, which could outcompete cyanobacteria under a relatively more turbulent regime due to their comparatively faster growth rates (Yu et al., 2018). These data suggest a strong link between $PC2_p$ and summer stratification strength, and $PC2_p$ follows the same overall downcore pattern exhibited by the turbulence-related $PC2_d$ (Figs. 4 and 6).

5.2. Ecological history of Lake Santiago and environmental forcing

Our multiproxy approach allows us to reconstruct the paleoecological evolution of the lake as a sequence of five coherent phases (Fig. 8).

Phase I (eutrophic lake, DAZs SAN-01 and SAN-02; ca. 1580–1870 CE)

This phase is characterized by the highest values of TOC in the entire record, a higher biomass of in-lake primary producers (β-carotene; Fig. 6), and dominance of the euplanktonic and eutrophic *A. granulata*. The TOC/TN_{corr} profile shows values between 10.58 and 17.25 for Unit 2 (average 13.78), indicating that the origin of the deposited organic matter, although lacustrine, was influenced by C3 land plants from the catchment (Meyers and Teranes, 2001). This is also supported by the high abundances of transported periphytic diatoms (Fig. 4). These data point to a lake largely influenced by the allochthonous delivery of nutrients, which probably drove a large part of its high primary production at the time.

The low values of $PC1_p$ suggest dominantly low N:P ratios favoring cyanobacteria and chlorophytes (Tilman et al., 1986). However, despite the minimum concentrations of diatoxanthin recorded throughout the core, it constitutes the most abundant pigment in the sediments (Fig. 6). The diatom assemblages are dominated by *A. granulata,* which, compared to other diatom taxa, have high P requirements (Kilham et al., 1986). The cooccurrence of the heavily silicified *A. granulata*, which requires a turbulent water regime to avoid sinking from the euphotic zone (Margalef, 1978a,b) and, by contrast, algal groups favored by thermal stratification, such as cyanobacteria, is also indicative of the existence of a eutrophic lake with marked seasonality (a very contrasting strong turbulent regime during springs vs. intensified stratification during the late summers).

The peak abundances of the eutrophic *Cyclotella meneghiniana* in DAZ SAN-02, at the expense of *A. granulata*, can be related to significant changes in the element stoichiometry of the water. *C. meneghiniana* is related to catchment disturbances (Roberts et al., 2016), and any excess delivery of P from the basin might significantly reduce Si availability due to elevated diatom production. Under these eutrophic circumstances, *C. meneghiniana* would benefit from lower Si:P ratios over the highly silicified *Aulacoseira* (Rühland et al., 2015; Tilman et al., 1982).

The geochemical, pigment, and diatom data describe a scenario of high nutrient availability during this phase. The potential intensification of erosion since Portuguese colonization deforested the landscape (Raposeiro et al., 2021), besides the dominant wet and warm conditions on the island at the time (Hernández et al., 2017, Fig. 8), explain the export of characteristically large amounts of P from watersheds of volcanic nature (Wetzel, 2001).

Phase II (mesotrophic lake, DAZ SAN-03; ca. 1870–1900 CE)

This phase shows a sharp change in diatom assemblages, dominated by the euplanktonic *A. ambigua*, suggesting a change to mesotrophic conditions with higher light:P and N:P ratios (e.g., Hassan, 2013; Kilham et al., 1986). The increase in the N:P ratio is also indicated by $PC1_p$. This change is accompanied by a strong decrease in both the abundance of periphytic diatoms and the TOC/TN_{corr} ratio (range 7.97–14.57, average 12.68), indicating a reduction in allochthonous inputs to the lake. The lack of aphanizophyll, a marker pigment of N_2-fixing cyanobacteria, also supports the interpretation of a higher N:P ratio. On the other hand, high values of $PC2_p$ indicate enhanced summer stratification, and this is compatible with the higher instrumental spring and summer (MAMJJA) maximum air temperature (MAT) record of Ponta Delgada at the time (Cropper and Hanna, 2014).

Phase III (eutrophic lake, DAZ SAN-04; ca. 1900–1930 CE)

This phase indicates a return to eutrophic conditions similar to Phase I, with TOC and in-lake primary production (β-carotene) showing quite similar recovery trends. The abundance of lutein also shows that chlorophytes replaced cyanobacteria during this phase. *A. granulata* reaches very high values, which, together with pigment data, suggests enhanced P availability under lower irradiance conditions (Kilham et al., 1986). However, the highly reduced numbers of periphytic diatoms and a forest-covered catchment at this time (Raposeiro et al., 2021; Rull et al., 2017) suggest that other causative factors of eutrophication, apart from external nutrient inputs, should be considered. Weakened stratification during the summer, as indicated by maximum values of $PC2_p$, is a major candidate, since it enhances internal P turnover, explaining the net increase in in-lake primary production (Wetzel, 2001). Moreover, meteorological data show a prolonged reduction in the spring and summer MATs during this phase (Fig. 8), which would, not only extend the mixing period, but also facilitate deeper mixing. Additionally, this phase also occurs after the stocking of cyprinid fish on the island, which could have altered top-down and bottom-up controls on primary production and lake food web dynamics (Buchaca et al., 2011; Raposeiro et al., 2017; Skov et al., 2010; Vázquez-Loureiro et al., 2019).

Vázquez-Loureiro et al. (2019). The percent abundances of *Aulacoseira granulata* and *Cyclotella meneghiniana* for Lake Santiago were recalculated once the allochthonous benthic diatom component was removed from the data matrix. For explanations on the meaning of the different proxies, see the text.

Phase IV (mesotrophic lake, DAZ SAN-05; ca. 1930–1990 CE)

The TOC/TN_{corr} ratio values are maintained during this phase, indicating the prevalence of lacustrine-dominated organic matter sedimentation. Pigment data show that primary production is dominated by diatoms, with a lower contribution of cyanobacteria, cryptophytes, and dinoflagellates. Lutein abruptly disappears at the beginning of this phase and occasionally reappears at very low concentrations, indicating that chlorophytes barely contributed to lake primary production. In addition, a new replacement of *A. granulata* by *A. ambigua* is recorded, suggesting a return to mesotrophic conditions similar to those of Phase II. Enhanced thermally-induced stratification is indicated by the high values of both the $PC2_p$ and the maximum spring and summer MATs at Ponta Delgada (Fig. 8).

Phase V (probable lake regime shift, DAZ SAN-06; ca. 1990–2011 CE)

This phase is characterized by a sharp shift in diatom species assemblages, with *Aulacoseira* being replaced mainly by *A. formosa* and, secondarily, by *F. crotonensis* and *F.* cf. *tenera*, resulting in maximum values for $PC2_d$. The change, therefore, points to enhanced stability of the water column, compatible with the increase in spring and summer MATs (Fig. 8). Diadinoxanthin (mainly characteristic of dinoflagellates) and alloxanthin (characteristic of cryptophytes) record their maximum values throughout the record, with diatoxanthin exhibiting a strong reduction in concentration. The greater contribution of motile groups, such as dinoflagellates and cryptophytes, at the expense of diatoms also indicates strengthened thermal stratification (Margalef, 1983). Oxygen depletion at the hypolimnion, promoting microbial anaerobic biomass, would explain the observed negative excursion in $\delta^{13}C_{org}$ values (Fig. 7) (Teranes and Bernasconi, 2005).

5.3. The different signatures of climate in the Sete Cidades deep lakes

Despite their proximity and, therefore, the same climatic context, the ecological histories of the two deep lakes in the Caldeira das Sete Cidades, Lake Santiago and Lake Azul (Fig. 1), show large differences in their responses to climate variability.

There is correspondence between the previously defined paleoclimate stages for São Miguel Island (Hernández et al., 2017), the meteorological data extending back to 1872 CE, and the predictable ecological responses of Lake Santiago, as explained in section 5.2 and shown in Fig. 8. The long-term climate changes in the island had two different effects on the ecological states of Lake Santiago: a) the wet and warm last stage of the LIA (Phase I) created the conditions for in-excess P delivery from the catchment, and b) the post-LIA (phases II to V) differences in the thermal structure of the water and, thus, in its mixing regime, induced by fluctuations in the spring and summer MATs. In this regard, thermal contact with the atmosphere imposes a temperature signal on the lake surface (Boehrer and Schultze, 2008), and spring and summer changes in the thermal structure of the water column are responsible for the different mixing regimes that alter the algal composition in lakes (Margalef, 1983).

Contrary to Lake Santiago, Lake Azul shows no direct correspondence with the São Miguel Island climate stages and/or changes in the spring and summer MATs mentioned above, except for the post-1980/90 CE period (Fig. 8). The catastrophic nature of the P17 eruption overrode the climatic signature in Lake Azul sediments due to the disruption of the biogeochemical cycling of nutrients (Vázquez-Loureiro et al., 2019). Tephra deposits create an impermeable barrier which can inhibit nutrient return, mainly P, from the sediments to the water column (Barker et al., 2000). In the case of thick tephra deposits, P-limitation due to massive tephra influx can have an impact on the long-term lake ontogeny, lasting up to millennia (Telford et al., 2004). Besides, the 16th century chronicles of Gaspar Frutuoso also show that more than two centuries after the P17 eruption, at least the area of the catchment adjacent to the lake was still made up of “sterile sands” (Frutuoso, 1977). Contrary to expectations, when this condition coincides with periods of enhanced runoff, the post-eruptive recovery of a volcanic lake can dramatically dilute any chemically enriched waters (Larson et al., 2006). Additionally, tephra deposition has the immediate effect of depauperating biological communities, restarting ecological succession. The periphytic algae characteristic of pioneering communities in oligotrophic lakes outcompete phytoplankton, because they can incorporate nutrients from both the water column and the sediments (Hansson, 1992). This mechanism could therefore also hinder the release of sufficient nutrients to support phytoplankton production (Vázquez-Loureiro et al., 2019). All these synergetic effects forced a long-term state of oligotrophy for ca. 650 yr (1290–1940 CE), only moderately modified by fish stocking and forestation practices and eventually interrupted by the extensive use of fertilizers. In contrast, the Lake Santiago sedimentary record shows that eutrophic conditions were present only 290 yr after the P17 catastrophic event.

This intersite comparison further confirms, at least for the studied proxies, the major site-specific component of the paleoenvironmental signal in these lakes. It can be hypothesized that the different effects of the regional (climatic) signal vs. site-specific ‘noise’ (Roberts et al., 2016) in lakes Azul vs. Santiago is a factor of both a) the closer distance of Lake Azul to the volcanic focus of the P17 eruption, which resulted in greater tephra fallout in Lake Azul than in Lake Santiago (Cole et al., 2008), and b) the large differences in the bathymetric and topographic gradients of both lakes and their catchments (Fig. 1), a factor that can play a critical role in altering the phototrophic response to climate variations (Gushulak et al., 2021). The latter can be partitioned into three main components, so that Lake Santiago, despite having, compared to Lake Azul, a similar depth (28.75 vs. 25.35 m) and lake area to catchment ratio (0.31 vs. 0.23) (Supplemental Table 1), shows 1) much steeper catchment slopes, 2) a water volume less than one order of magnitude, and 3) a simple bathymetry without planar surfaces which facilitates more linear responses (Stone and Fritz, 2004; Bao et al., 2015). These factors together would not only promote a larger nutrient inwash to Lake Santiago, but also amplify the effects of variations in catchment-mediated climate forcings in this much smaller deep lake compared to Lake Azul. As a result, the sediments of Lake Azul fail as a reliable archive of changes in climate conditions in the archipelago for the selected proxy-based records at the considered temporal scale.

5.4. The post-1980 CE climate forcing scenario in the Sete Cidades deep lakes

The almost synchronous and identical major post-1980 CE shift in Lake Azul and Lake Santiago's diatom assemblages suggests a common underlying control at the regional scale.

The complete implications of global warming for lake systems are still largely unresolved, including the restructuring of diatom communities. According to several sediment studies, global warming is forcing widespread diatom assemblage shifts by altering thermal lake properties (e.g., Hadley et al., 2019; Rühland et al., 2015; Sivarajah et al., 2016; Sorvari et al., 2002). Other studies stress that an accelerated nutrient increase in recent decades, such as by atmospheric N_2 deposition, is another critical

driver shifting diatom assemblages (e.g., Dong et al., 2012; Hu et al., 2014; Wolfe et al., 2013).

The simultaneous replacement of *Aulacoseira* spp. As the dominant taxon in Lake Santiago and Lake Azul involves the expansion of *A. formosa*, *F. crotonensis* and *F.* cf. *tenera* (Fig. 4 and Supplementary Fig. 3). Enhanced atmospheric N_2 deposition could be responsible for the widespread increases in the relative abundance of *A. formosa* and *F. crotonensis* in recent decades (e.g., Saros et al., 2005). This nutrient enrichment is manifested in the sedimentary records by a sustained 20th century decline in $\delta^{15}N_{org}$ and a %N increase (Wolfe et al., 2006, 2013). However, there is no evidence of a clear net negative trend in $\delta^{15}N_{org}$, as there is a lack of %N enrichment, in Lake Santiago (Fig. 7 and Supplementary Fig. 3). The post-1985 CE record of Lake Santiago shows negligible increases in TOC and TN in the uppermost sediments. The same is true for β-carotene, an indicator of total algal biomass (Buchaca et al., 2019; Leavitt and Hodgson, 2001, Fig. 6). Nutrient enrichment associated with land clearance as a likely cause for the *A. formosa* increase (e.g., Boeff et al., 2016) can therefore also be disregarded. Additionally, the high light requirements of *F. crotonensis* (Interlandi et al., 1999) are not compatible with a scenario involving turbid waters produced by eutrophication.

As a result, changes in nutrient concentrations are unlikely factors driving diatom community changes in Lake Santiago in recent decades. Alternatively, a shift in thermal properties of the water column could be the causative factor for the replacement of the *Aulacoseira*-vs. *Asterionella*- and *Fragilaria*-dominated fossil assemblages. Thick-walled cells, such as those of *Aulacoseira* spp., require well-mixed water column conditions to avoid sinking out from the euphotic zone (Margalef, 1978a,b). The worldwide reduction of their abundances in recent sediments has been considered indicative of increased water column stability associated with warmer climate conditions (Rühland et al., 2008, 2015) In contrast, the elongated shape and/or colonial capabilities of species such as *A. formosa*, *F. crotonensis* and *F. tenera* are key adaptations that decelerate their sinking velocities, allowing these species to thrive in prevailing stratification regimes (Reynolds, 2006). Such changes in the thermal lake properties would also explain the peak abundances of motile phytoplankton, such as dinoflagellates (diadinoxanthin) and cryptophytes (alloxanthin). Moreover, the recent net negative trend in $\delta^{13}C_{org}$ values could also be likely caused by the proliferation of anaerobic bacteria occurring under the anoxia induced by prolonged and/or intensified thermal water stratification conditions.

The shift in diatom community structure in Lake Santiago in recent decades resembles that of mesotrophic lakes where warmer climates favor those species making the best trade-off between decreasing nutrients and increased water column stability (Berthon et al., 2014). Both *A. formosa* and *F. crotonensis* are favored by relatively high N:P and Si:P ratios (Interlandi et al., 1999; Saros et al., 2005), and *F. tenera* by low P (Interlandi et al., 1999) and high temperatures (Kienel et al., 2005), so the three taxa would fulfill those requirements. The timing of this turnover in diatom species composition is consistent with the records of Lake Azul (Vázquez-Loureiro et al., 2019) and Lake Empadadas (Marques, 2021). It is also compatible with the available environmental monitoring data of other lakes in the archipelago, such as Lake Furnas and Lake Fogo, where a shift to *Asterionella*- and *Fragilaria*-dominated assemblages has been observed (Gonçalves, 2008), despite the large local-scale differences among these systems. However, this local component still plays its own significant role. There are notable differences in the type of response, gradual in Lake Azul vs. abrupt in Lake Santiago (Supplementary Fig. 3), related to differences in the size and morphometry of each lake. Large lakes, such as Lake Azul, compared to Lake Santiago, have deeper mixing depths (Hanna, 1990; Gillis et al., 2021), longer cooling periods (Nürnberg, 1988), and a more poorly developed thermocline (Oswald and Rouse, 2004) than smaller lakes. These characteristics make larger lakes require extra warming related to their larger water volumes (Gillis et al., 2021), so a threshold response of biotic communities is more likely in Lake Santiago where, with approximately. One order of magnitude less volume (Supplemental Table 1), heating up the epilimnion requires less energy.

6. Conclusions

Despite the proximity of the studied lakes, our results demonstrate pronounced differences in the sensitivity of the two deep temperate volcanic lakes under equal climate forcing. From ca. 1580 CE and until ca. 1980/90 CE, the long-term ecological trajectory of the small Lake Santiago was mainly determined by climate variability. In contrast, other natural (volcanism) and nonnatural (reforestation, invasive species introduction and artificial fertilization) environmental drivers played a much larger role in the evolution of the large Lake Azul. The reconstructed ecological history of Lake Santiago, based on a multiproxy approach, reveals that since ca. 1580 CE, the lake has experienced ecological shifts in phase with the major climate stages known for São Miguel Island.

During the last warm and wet stage of the LIA (1580–1870 CE), high P availability linked to runoff resulted in eutrophic conditions, characterized by the dominance of the diatom *A. granulata*, negligible presence of mesotrophic *A. ambigua*, and peak abundances of cyanobacteria. The shifting dominance of *A. granulata* vs. mesotrophic *A. ambigua* characterizes the post-LIA ecological history of the lake, and it was related to the maximum spring and summer atmospheric temperature variability, which provoked changes in the mixing regime. Higher temperatures induced a more stable water column during the 1870–1900 CE and 1930–1960 CE periods, with the dominance of *A. ambigua* and a higher relative contribution of cyanobacteria over chlorophytes in the plankton. Conversely, reduced temperatures in the 1900–1930 CE period favored deeper mixing, which benefited *A. granulata* over *A. ambigua*, as well as chlorophytes.

An intersite comparison with Lake Azul, located just 2.5 km away inside the caldera, showed major differences in the ecological response preserved in the sedimentary record under the same climate scenario until ca. 1980/90 CE. A disruption of biogeochemical cycles after the massive deposition of tephra induced by a catastrophic volcanic eruption in ca. 1290 CE masked the climate signature in the sedimentary record.

Despite this multistressor scenario, the post-1980/90 CE period showed a probable ecological regime shift in both lakes – also shown by the current limnological monitoring programs of other lakes on São Miguel Island – triggered by higher water temperatures under global warming conditions.

This demonstration of different long-term responses to climate variability in these close-proximity lakes not only implies that they register dissimilar information for paleoclimate research but also has management implications for the preservation of ecosystem services. The magnitude and pattern of response in the post-1980/90 CE period involve a disruptive and large replacement of turbulence-loving diatoms by taxa favoring warm stratified waters in Lake Santiago, and a similar change occurred in Lake Azul, although more gradual and less pronounced. This suggests that, despite their similarities and being forced by the same climate conditions, the two lakes require the adoption of different management strategies under the current climate change scenario, with Lake Santiago being more vulnerable to the effects of global warming and Lake Azul being more resilient.

Author contributions

All authors contributed to the manuscript and approved submission. DV-L and RB conducted the research, analyzed the diatom samples, processed and interpreted the data, made the tables and figures and wrote the manuscript; AS described the lithofacies, performed the stratigraphic correlations and interpreted data; VG reviewed the diatom taxonomy and processed and interpreted the data; TB analyzed the pigment data and processed and interpreted the data; AH processed and interpreted the (paleo)climate data; PR processed and interpreted the data; EdB contributed pollen data for the age–depth model; and PM contributed ^{210}Pb and ^{137}Cs data for the age–depth model. VG, AS, AH, SG, PR and RB cored the lake. All authors revised the manuscript. AS, SG and RB led the research.

Funding

This research was funded by the Spanish Ministry of Economy and Competitiveness projects PaleoNAO, RapidNAO and PaleoModes (CGL 2010-15767, CGL 2013-40608-R and CGL 2016-75281-C2, respectively) and by the Fundação para a Ciência e Tecnologia (PTDC/CTA-AMB/28,511/2017). David Vázquez-Loureiro, Armand Hernández, and Pedro Raposeiro benefited with grants from the Xunta de Galicia (I2C Programme co-funded with the European Social Fund), the Spanish Ministry of Science and Innovation through the Ramón y Cajal Scheme [RYC 2020-029253-I], and Fundação para a Ciência e Tecnologia (DL57/2016/ICETA/EEC 2018/25), respectively. Funding for open access charge: Universidade da Coruña/CISUG.

Declaration of competing interest

The authors declare that they have no known competing financial interests or personal relationships that could have appeared to influence the work reported in this paper.

Data availability

Data will be made available on request.

Acknowledgements

We thank María Jesús Rubio, Olga Margalef and Guiomar Sánchez-López for field assistance. The IAEA is grateful for the support provided to its Marine Environment Laboratories by the Government of the Principality of Monaco. Our thanks are also extended to two anonymous reviewers for their very useful and constructive comments on an earlier version of the manuscript.

Appendix A. Supplementary data

Supplementary data to this article can be found online at https://doi.org/10.1016/j.quascirev.2023.107968.

References

Andersen, T., Carstensen, J., Hernández-García, E., Duarte, C.M., 2009. Ecological thresholds and regime shifts: approaches to identification. Trends Ecol. Evol. 24, 49–57. https://doi.org/10.1016/j.tree.2008.07.014.

Andrade, C., Cruz, J.V., Viveiros, F., Coutinho, R., 2019. CO_2 flux from volcanic lakes in the western group of the Azores Archipelago (Portugal). Water 11, 599. https://doi.org/10.3390/w11030599.

Andrade, C., Trigo, R.M., Freitas, M.C., Gallego, M.C., Borges, P., Ramos, A.M., 2008. Comparing historic records of storm frequency and the North Atlantic Oscillation (NAO) chronology for the Azores region. Holocene 18, 745–754. https://doi.org/10.1177/0959683608091794.

Andrade, M., Ramalho, R.S., Pimentel, A., Hernández, A., Kutterolf, S., Sáez, A., Benavente, M., Raposeiro, P.M., Giralt, S., 2021. Unraveling the Holocene eruptive history of Flores Island (Azores) through the analysis of lacustrine sedimentary records. Front. Earth Sci. 9, 889. https://doi.org/10.3389/feart.2021.738178.

Appleby, P.G., 2001. Chronostratigraphic techniques in recent sediments. In: Last, W.M., Smol, J.P. (Eds.), Tracking Environmental Change Using Lake Sediments: Volume 1: Basin Analysis, Coring, and Chronological Techniques. Kluwer Academic Publishers, Dordrecht, Netherlands, pp. 171–203.

Bao, R., Hernández, A., Sáez, A., Giralt, S., Prego, R., Pueyo, J.J., Moreno, A., Valero-Garcés, B.L., 2015. Climatic and lacustrine morphometric controls of diatom paleoproductivity in a tropical Andean lake. Quat. Sci. Rev. 129, 96–110. https://doi.org/10.1016/j.quascirev.2015.09.019.

Bao, R., Sáez, A., Servant-Vildary, S., Cabrera, L., 1999. Lake-level and salinity reconstruction from diatom analyses in Quillagua formation (late Neogene, Central Andean forearc, Northern Chile). Palaeogeogr. Palaeoclimatol. Palaeoecol. 153, 309–335. https://doi.org/10.1016/S0031-0182(99)00066-8.

Barker, P., Telford, R., Merdaci, O., Williamson, D., Taieb, M., Vincens, A., Gibert, E., 2000. The sensitivity of a Tanzanian crater lake to catastrophic tephra input and four millennia of climate change. The Holocene 10, 303–310. https://doi.org/10.1191/095968300672848582.

Bennett, K.D., 1996. Determination of the number of zones in a biostratigraphical sequence. New Phytol. 132, 155–170. https://doi.org/10.1111/j.1469-8137.1996.tb04521.x.

Bennett, K.D., 2002. Documentation for Psimpoll 4.10 and Pscomb 1.03. C Programs for Plotting Pollen Diagrams and Analysing Pollen Data. Uppsala University, Uppsala, Sweden.

Berthon, V., Alric, B., Rimet, F., Perga, M.-E., 2014. Sensitivity and responses of diatoms to climate warming in lakes heavily influenced by humans. Freshw. Biol. 59, 1755–1767. https://doi.org/10.1111/fwb.12380.

Boeff, K.A., Strock, K.E., Saros, J.E., 2016. Evaluating planktonic diatom response to climate change across three lakes with differing morphometry. J. Paleolimnol. 56, 33–47. https://doi.org/10.1007/s10933-016-9889-z.

Boehrer, B., Schultze, M., 2008. Stratification of lakes. Rev. Geophys. 46, RG2005. https://doi.org/10.1029/2006RG000210.

Buchaca, T., Catalan, J., 2007. Factors influencing the variability of pigments in the surface sediments of mountain lakes. Freshw. Biol. 52, 1365–1379. https://doi.org/10.1111/j.1365-2427.2007.01774.x.

Buchaca, T., Catalan, J., 2008. On the contribution of phytoplankton and benthic biofilms to the sediment record of marker pigments in high mountain lakes. J. Paleolimnol. 40, 369–383. https://doi.org/10.1007/s10933-007-9167-1.

Buchaca, T., Kosten, S., Lacerot, G., Mazzeo, N., Kruk, C., Huszar, V.L.M., Lotter, A.F., Jeppesen, E., 2019. Pigments in surface sediments of South American shallow lakes as an integrative proxy for primary producers and their drivers. Freshw. Biol. 64, 1437–1452. https://doi.org/10.1111/fwb.13317.

Buchaca, T., Skov, T., Amsinck, S.L., Gonçalves, V., Azevedo, J.M.N., Andersen, T.J., Jeppesen, E., 2011. Rapid ecological shift following piscivorous fish introduction to increasingly eutrophic and warmer lake furnas (Azores Archipelago, Portugal): a Paleoecological Approach. Ecosystems 14, 458–477. https://doi.org/10.1007/s10021-011-9423-0.

Cole, P.D., Pacheco, J.M., Gunasekera, R., Queiroz, G., Gonçalves, P., Gaspar, J.L., 2008. Contrasting styles of explosive eruption at Sete Cidades, São Miguel, Azores, in the last 5000 years: hazard implications from modelling. J. Volcanol. Geoth. Res. 178, 574–591. https://doi.org/10.1016/j.jvolgeores.2008.01.008.

Cropper, T.E., Hanna, E., 2014. An analysis of the climate of Macaronesia, 18652012. Int. J. Climatol. 34, 604–622. https://doi.org/10.1002/joc.3710.

De Albergaria, I.S., 2000. Quintas, jardins e parques da ilha de Sao Miguel, (1785-1885). Quetzal Editores, Lisbon, Portugal.

Dong, X., Bennion, H., Maberly, S.C., Sayer, C.D., Simpson, G.L., Battarbee, R.W., 2012. Nutrients exert a stronger control than climate on recent diatom communities in Esthwaite water: evidence from monitoring and palaeolimnological records. Freshw. Biol. 57, 2044–2056. https://doi.org/10.1111/j.1365-2427.2011.02670.x.

Frutuoso, G., 1977. Livro Quarto das Saudades da Terra. Instituto Cultural de Ponta Delgada, Ponta Delgada, Azores, Portugal.

Gillis, D.P., Minns, C.K., Shuter, B.J., 2021. Predicting open-water thermal regimes of temperate North American lakes. Can. J. Fish. Aquat. Sci. 78, 820–840. https://doi.org/10.1139/cjfas-2020-0140.

Gonçalves, V., 2008. Contribuçao para o Estudo da Qualidade Ecológica das Lagoas dos Açores. Fitoplâncton e Diatomáceas Bentónicas. PhD. Dissertation. Universidade dos Açores (Ponta Delgada, Portugal).

Goncalves, V., Marques, H., Fonseca, A., 2010. Lista das diatomáceas (Bacillariophyta). In: Borges, P.A.V., Bried, J., Costa, A., Cunha, R., Gabriel, R., Goncalves, V., Martins, A.F., Melo, I., Parente, M., Raposeiro, P., Rodrigues, P., Santos, R.S., Silva, L., Vieira, P., Vieira, V. (Eds.), Listagem Dos Organismos Terrestres e Marinhos Dos Acores. Princípia, Cascais, Portugal, pp. 81–97.

Grimm, E.C., 1987. CONISS: a FORTRAN 77 program for stratigraphically constrained cluster analysis by the method of incremental sum of squares. Comput. Geosci. 13, 13–35. https://doi.org/10.1016/0098-3004(87)90022-7.

Gushulak, C.A.C., Leavitt, P.R., Cumming, B.F., 2021. Basin-specific records of lake oligotrophication during the middle-to-late Holocene in boreal northeast Ontario, Canada. Holocene 31, 1539–1554. https://doi.org/10.1177/09596836211025972.

Hadley, K.R., Paterson, A.M., Rühland, K.M., White, H., Wolfe, B.B., Keller, W., Smol, J.P., 2019. Biological and geochemical changes in shallow lakes of the Hudson Bay Lowlands: a response to recent warming. J. Paleolimnol. 61, 313–328. https://doi.org/10.1007/s10933-018-0061-9.

Hanna, M., 1990. Evaluation of models predicting mixing depth. Can. J. Fish. Aquat. Sci. 47, 940–947. https://doi.org/10.1139/f90-108.
Hansson, L.-A., 1992. Factors regulating periphytic algal biomass. Limnol. Oceanogr. 37, 322–328. https://doi.org/10.4319/lo.1992.37.2.0322.
Hargan, K.E., Nelligan, C., Jeziorski, A., Rühland, K.M., Paterson, A.M., Keller, W., Smol, J.P., 2016. Tracking the long-term responses of diatoms and cladocerans to climate warming and human influences across lakes of the Ring of Fire in the Far North of Ontario, Canada. J. Paleolimnol. 56, 153–172. https://doi.org/10.1007/s10933-016-9901-7.
Hassan, G.S., 2013. Diatom-based reconstruction of middle to late holocene paleoenvironments in Lake Lonkoy, southern Pampas, Argentina. Diatom Res. 28, 473–486. https://doi.org/10.1080/0269249X.2013.851118.
Hernández, A., Bao, R., Giralt, S., Leng, M.J., Barker, P.A., Sáez, A., Pueyo, J.J., Moreno, A., Valero-Garcés, B.L., Sloane, H.J., 2008. The palaeohydrological evolution of Lago Chungará (Andean Altiplano, Northern Chile) during the Lateglacial and early Holocene using oxygen isotopes in diatom silica. J. Quat. Sci. 23, 351–363. https://doi.org/10.1002/jqs.1173.
Hernández, A., Kutiel, H., Trigo, R.M., Valente, M.A., Sigró, J., Cropper, T., Santo, F.E., 2016. New Azores Archipelago daily precipitation dataset and its links with large-scale modes of climate variability. Int. J. Climatol. 36, 4439–4454. https://doi.org/10.1002/joc.4642.
Hernández, A., Martin-Puertas, C., Moffa-Sánchez, P., Moreno-Chamarro, E., Ortega, P., Blockley, S., Cobb, K.M., Comas-Bru, L., Giralt, S., Goosse, H., Luterbacher, J., Martrat, B., Muscheler, R., Parnell, A., Pla-Rabes, S., Sjolte, J., Scaife, A.A., Swingedouw, D., Wise, E., Xu, G., 2020. Modes of climate variability: synthesis and review of proxy-based reconstructions through the Holocene. Earth Sci. Rev. 209, 103286. https://doi.org/10.1016/j.earscirev.2020.103286.
Hernández, A., Sáez, A., Bao, R., Raposeiro, P.M., Trigo, R.M., Doolittle, S., Masqué, P., Rull, V., Gonçalves, V., Vázquez-Loureiro, D., Rubio-Inglés, M.J., Sánchez-López, G., Giralt, S., 2017. The influences of the AMO and NAO on the sedimentary infill in an Azores Archipelago lake since ca. 1350CE. Global Planet. Change 154, 61–74. https://doi.org/10.1016/j.gloplacha.2017.05.007.
Houk, V., Klee, R., 2007. Atlas of freshwater centric diatoms with a brief key and descriptions. Part II. Melosiraceae and Aulacoseiraceae (Supplement to Part I). Fottea 7, 85–255.
Hu, Z., Anderson, N.J., Yang, X., McGowan, S., 2014. Catchment-mediated atmospheric nitrogen deposition drives ecological change in two alpine lakes in SE Tibet. Global Change Biol. 20, 1614–1628. https://doi.org/10.1111/gcb.12435.
Interlandi, S.J., Kilham, S.S., Theriot, E.C., 1999. Responses of phytoplankton to varied resource availability in large lakes of the Greater Yellowstone Ecosystem. Limnol. Oceanogr. 44, 668–682. https://doi.org/10.4319/lo.1999.44.3.0668.
Jackson, S.T., Hobbs, R.J., 2009. Ecological restoration in the light of ecological history. Science 325, 567–569. https://doi.org/10.1126/science.1172977.
Jeffers, E.S., Nogué, S., Willis, K.J., 2015. The role of palaeoecological records in assessing ecosystem services. Quat. Sci. Rev. 112, 17–32. https://doi.org/10.1016/j.quascirev.2014.12.018.
Jeffrey, S.W., Mantoura, R.F.C., Wright, S.W., 1997. Phytoplankton Pigments in Oceanography: Guidelines to Modern Methods. UNESCO Publishing, Paris, France.
Jovanelly, T.J., Fritz, S.C., 2011. Morphometric and chemical response of two contrasting lake systems to modern climate change. J. Paleolimnol. 46, 89–98. https://doi.org/10.1007/s10933-011-9521-1.
Keegan, W.F., Diamond, J.M., 1987. Colonization of islands by humans: a biogeographical perspective. In: Schiffer, M.B. (Ed.), Advances in Archaeological Method and Theory. Academic Press, San Diego, CA, pp. 49–92.
Kienel, U., Schwab, M.J., Schettler, G., 2005. Distinguishing climatic from direct anthropogenic influences during the past 400 years in varved sediments from Lake Holzmaar (Eifel, Germany). J. Paleolimnol. 33, 327–347. https://doi.org/10.1007/s10933-004-6311-z.
Kilham, P., Kilham, S.S., Hecky, R.E., 1986. Hypothesized resource relationships among African planktonic diatoms. Limnol. Oceanogr. 31, 1169–1181. https://doi.org/10.4319/lo.1986.31.6.1169.
Krammer, K., Lange-Bertalot, H., 1986-1991. Bacillariophyceae. In: Ettl, H., Gerloff, J., Heynig, H., Mollenhauer, D. (Eds.), Sußwasserflora von Mitteleuropa. Fischer-Verlag, Stuttgart.
Krammer, K., 2000. Diatoms of the European Inland Waters and Comparable Habitats. Volume 1. In: The Genus *Pinnularia*, Diatoms of the European Inland Waters and Comparable Habitats. Volume 1. A. R. G. Gantner Verlag, Ruggell, Liechtenstein, p. 703.
Krammer, K., 2002. Diatoms of the European inland waters and comparable habitats. Volume 3. *Cymbella*. In: Lange-Bertalot, H. (Ed.), Diatoms of the European Inland Waters and Comparable Habitats, Volume 3. A. R. A. Gantner Verlag, Ruggell, Liechtenstein, p. 584.
Krammer, K., 2003. Diatoms of the European inland waters and comparable habitats. Volume 4. *Cymbopleura, Delicata, Navicymbula, Gomphocymbellopsis, Afrocymbella*. In: Lange-Bertalot, H. (Ed.), Diatoms of the European Inland Waters and Comparable Habitats, Volume 4. A. R. A. Gantner Verlag, Ruggell, Liechtenstein, p. 530.
Lange-Bertalot, H., 2001. Diatoms of the European inland waters and comparable habitats. Volume 2. *Navicula sensu stricto*, 10 genera separated from *Navicula sensu lato*, *Frustulia*. In: Lange-Bertalot, H. (Ed.), Diatoms of the European Inland Waters and Comparable Habitats, Volume 2. A. R. G. Gantner Verlag, Ruggell, Liechtenstein, p. 526.
Lange-Bertalot, H., Bak, M., Witkowski, A., 2011. Diatoms of the European inland waters and comparable habitats. Volume 6. *Eunotia* and some related genera. In: Lange-Bertalot, H. (Ed.), Diatoms of the European Inland Waters and Comparable Habitats, ume 6. A. R. G. Gantner Verlag, Ruggell, Liechtenstein, p. 747.
Lange-Bertalot, H., Ulrich, S., 2014. Contributions to the taxonomy of needle-shaped *Fragilaria* and *Ulnaria* species. Lauterbornia 78, 1–73.
Larson, D.W., Sweet, J., Petersen, R.R., Crisafulli, C.M., 2006. Posteruption response of phytoplankton and zooplankton communities in spirit lake, mount st. Helens, Washington. Lake reserv. OR Manag. 22, 273–292. https://doi.org/10.1080/07438140609354362.
Leavitt, P.R., Fritz, S.C., Anderson, N.J., Baker, P.A., Blenckner, T., Bunting, L., Catalan, J., Conley, D.J., Hobbs, W.O., Jeppesen, E., Korhola, A., McGowan, S., Rühland, K., Rusak, J.A., Simpson, G.L., Solovieva, N., Werne, J., 2009. Paleolimnological evidence of the effects on lakes of energy and mass transfer from climate and humans. Limnol. Oceanogr. 54, 2330–2348. https://doi.org/10.4319/lo.2009.54.6_part_2.2330.
Leavitt, P.R., Hodgson, D., 2001. Sedimentary pigments. In: Smol, J., Birks, H., Last, M. (Eds.), Tracking Environmental Change Using Lake Sediments Volume 3: Terrestrial, Algal, and Siliceous Indicators. Kluwer Academic Press, Dordrecht, Netherlands, pp. 295–326.
Levkov, Z., 2009. Diatoms of the European inland waters and comparable habitats. Volume 5. *Amphora sensu lato*. In: Lange-Bertalot, H. (Ed.), Diatoms of the European Inland Waters and Comparable Habitats, Volume 4. A. R. A. Gantner Verlag, Ruggell, Liechtenstein, p. 916.
Levkov, Z., Metzeltin, D., Pavlov, A., 2013. Diatoms of the European inland waters and comparable habitats. Volume 7. *Luticola* and *luticulopsis*. In: Lange-Bertalot, H. (Ed.), Diatoms of the European Inland Waters and Comparable Habitats, ume 7. A. R. A. Gantner Verlag, Ruggell, Liechtenstein, p. 698.
Louys, J., 2012. Paleontology in Ecology and Conservation: Springer Earth System Sciences. Springer Science & Business Media, Berlin, Germany.
Margalef, R., 1978a. Life-forms of phytoplankton as survival alternatives in an unstable environment. Oceanol. Acta 1, 493–509.
Margalef, R., 1978b. Phytoplankton communities in upwelling areas. The example of NW Africa. Oceanol. Aquat. 3, 97–132.
Margalef, R., 1983. Limnología. Ediciones Omega, Barcelona, Spain.
Marques, H.S., 2021. Reconstruction of Past Environmental Changes in the Azores Based on Lacustrine Diatom Sedimentary Records. Universidade dos Açores, Azores, Portugal.
Meyers, P.A., Teranes, J.L., 2001. Sediment organic matter. In: Smol, J.P., Birks, H.J.B., Last, W.M. (Eds.), Tracking Environmental Change Using Lake Sediments. Volume 2: Physical and Geochemical Methods. Kluwer Academic Publishers, Dordrecht, Netherlands, pp. 239–269.
Mills, K., Schillereff, D., Saulnier-Talbot, É., Gell, P., Anderson, N.J., Arnaud, F., Dong, X., Jones, M., McGowan, S., Massaferro, J., Moorhouse, H., Perez, L., Ryves, D.B., 2017. Deciphering long-term records of natural variability and human impact as recorded in lake sediments: a palaeolimnological puzzle. WIREs Water 4, e1195. https://doi.org/10.1002/wat2.1195.
Nogué, S., Santos, A.M.C., Birks, H.J.B., Björck, S., Castilla-Beltrán, A., Connor, S., de Boer, E.J., de Nascimento, L., Felde, V.A., Fernández-Palacios, J.M., Froyd, C.A., Haberle, S.G., Hooghiemstra, H., Ljung, K., Norder, S.J., Peñuelas, J., Prebble, M., Stevenson, J., Whittaker, R.J., Willis, K.J., Wilmshurst, J.M., Steinbauer, M.J., 2021. The human dimension of biodiversity changes on islands. Science 372, 488–491. https://doi.org/10.1126/science.abd6706.
Nürnberg, G.K., 1988. Prediction of phosphorus release rates from total and reductant-soluble phosporus in anoxic lake-sediments. Can. J. Fish. Aquat. Sci. 45, 453–462. https://doi.org/10.1139/f88-054.
Oswald, C.J., Rouse, W., 2004. Thermal characteristics and energy balance of various-size Canadian shield lakes in the Mackenzie river basin. J. Hydrometeorol. 5, 129–144.
Potapova, M.G., Bixby, R.J., Charles, D.F., Edlund, M.B., Enache, M.E., Furey, P., Hamilton, P.B., Lowe, R.L., Manoylov, K.M., Ognjanova-Rumenova, N., Ponader, K.C., Ren, L., Siver, P.A., Spaulding, S.A., Zalack, J., 2008. Representatives of the Genus *Aulacoseira* Thwaites in NAWQA, Eighteenth NAWQA Workshop on Harmonization of Algal Taxonomy. The Academy of Natural Sciences of Philadelphia, Philadelphia. April 27-29, 2007.
Pereira, C.L., Raposeiro, P.M., Costa, A.C., Bao, R., Giralt, S., Gonçalves, V., 2014. Biogeography and lake morphometry drive diatom and chironomid assemblages' composition in lacustrine surface sediments of oceanic islands. Hydrobiologia 730, 93–112. https://doi.org/10.1007/s10750-014-1824-6.
Queiroz, G., 1997. Vulcão das Sete Cidades (S. Miguel, Açores): História Eruptiva e Avaliação do Hazard. PhD Thesis. Universidade dos Açores. Departamento de Geociências.
Queiroz, G., Pacheco, J.M., Gaspar, J.L., Aspinall, W.P., Guest, J.E., Ferreira, T., 2008. The last 5000 years of activity at Sete Cidades volcano (São Miguel island, Azores): implications for hazard assessment. J. Volcanol. Geoth. Res. 178, 562–573. https://doi.org/10.1016/j.jvolgeores.2008.03.001.
Raposeiro, P.M., Hernández, A., Pla-Rabes, S., Gonçalves, V., Bao, R., Sáez, A., Shanahan, T., Benavente, M., de Boer, E.J., Richter, N., Gordon, V., Marques, H., Sousa, P.M., Souto, M., Matias, M.G., Aguiar, N., Pereira, C., Ritter, C., Rubio, M.J., Salcedo, M., Vázquez-Loureiro, D., Margalef, O., Amaral-Zettler, L.A., Costa, A.C., Huang, Y., van Leeuwen, J.F.N., Masqué, P., Prego, R., Ruiz-Fernández, A.C., Sánchez-Cabeza, J.-A., Trigo, R., Giralt, S., 2021. Climate change facilitated the early colonization of the Azores Archipelago during medieval times. Proc. Natl. Acad. Sci. U.S.A. 118, e2108236118. https://doi.org/10.1073/pnas.2108236118.
Raposeiro, P.M., Rubio, M.J., González, A., Hernández, A., Sánchez-López, G., Vázquez-Loureiro, D., Rull, V., Bao, R., Costa, A.C., Gonçalves, V., Sáez, A., Giralt, S., 2017. Impact of the historical introduction of exotic fishes on the

chironomid community of Lake Azul (Azores Islands). Palaeogeogr. Palaeoclimatol. Palaeoecol. 466, 77–88. https://doi.org/10.1016/j.palaeo.2016.11.015.
Raposeiro, P.M., Sáez, A., Giralt, S., Costa, A.C., Gonçalves, V., 2018. Causes of spatial distribution of subfossil diatom and chironomid assemblages in surface sediments of a remote deep island lake. Hydrobiologia 815, 141–163. https://doi.org/10.1007/s10750-018-3557-4.
Reimer, P.J., Bard, E., Bayliss, A., Beck, J.W., Blackwell, P.G., Ramsey, C.B., Buck, C.E., Cheng, H., Edwards, R.L., Friedrich, M., Grootes, P.M., Guilderson, T.P., Haflidason, H., Hajdas, I., Hatté, C., Heaton, T.J., Hoffmann, D.L., Hogg, A.G., Hughen, K.A., Kaiser, K.F., Kromer, B., Manning, S.W., Niu, M., Reimer, R.W., Richards, D.A., Scott, E.M., Southon, J.R., Staff, R.A., Turney, C.S.M., van der Plicht, J., 2013. IntCal13 and marine13 radiocarbon age calibration curves 0–50,000 years cal BP. Radiocarbon 55, 1869–1887. https://doi.org/10.2458/azu_js_rc.55.16947.
Renberg, I., 1990. A procedure for preparing large sets of diatom slides from sediment cores. J. Paleolimnol. 4, 87–90. https://doi.org/10.1007/BF00208301.
Reynolds, C.S., 2006. The Ecology of Phytoplankton. Cambridge University Press, Cambridge, NY.
Richter, N., Russell, J.M., Amaral-Zettler, L., DeGroff, W., Raposeiro, P.M., Gonçalves, V., de Boer, E.J., Pla-Rabes, S., Hernández, A., Benavente, M., Ritter, C., Sáez, A., Bao, R., Trigo, R.M., Prego, R., Giralt, S., 2022. Long-term hydroclimate variability in the sub-tropical North Atlantic and anthropogenic impacts on lake ecosystems: a case study from Flores Island, the Azores. Quat. Sci. Rev. 285, 107525. https://doi.org/10.1016/j.quascirev.2022.107525.
Ritter, C., Gonçalves, V., Pla-Rabes, S., de Boer, E.J., Bao, R., Sáez, A., Hernández, A., Sixto, M., Richter, N., Benavente, M., Prego, R., Giralt, S., Raposeiro, P.M., 2022. The vanishing and the establishment of a new ecosystem on an oceanic island – anthropogenic impacts with no return ticket. Sci. Total Environ. 830, 154828. https://doi.org/10.1016/j.scitotenv.2022.154828.
Roberts, N., Allcock, S.L., Arnaud, F., Dean, J.R., Eastwood, W.J., Jones, M.D., Leng, M.J., Metcalfe, S.E., Malet, E., Woodbridge, J., Yiğitbaşıoğlu, H., 2016. A tale of two lakes: a multi-proxy comparison of Lateglacial and Holocene environmental change in Cappadocia, Turkey. J. Quat. Sci. 31, 348–362. https://doi.org/10.1002/jqs.2852.
Rühland, K., Paterson, A.M., Smol, J.P., 2008. Hemispheric-scale patterns of climate-related shifts in planktonic diatoms from North American and European lakes. Global Change Biol. 14, 2740–2754. https://doi.org/10.1111/j.1365-2486.2008.01670.x.
Rühland, K.M., Paterson, A.M., Smol, J.P., 2015. Lake diatom responses to warming: reviewing the evidence. J. Paleolimnol. 54, 1–35. https://doi.org/10.1007/s10933-015-9837-3.
Rull, V., Lara, A., Rubio-Inglés, M.J., Giralt, S., Gonçalves, V., Raposeiro, P., Hernández, A., Sánchez-López, G., Vázquez-Loureiro, D., Bao, R., Masqué, P., Sáez, A., 2017. Vegetation and landscape dynamics under natural and anthropogenic forcing on the Azores Islands: a 700-year pollen record from the São Miguel Island. Quat. Sci. Rev. 159, 155–168. https://doi.org/10.1016/j.quascirev.2017.01.021.
Sáez, A., Valero-Garcés, B.L., Giralt, S., Moreno, A., Bao, R., Pueyo, J.J., Hernández, A., Casas, D., 2009. Glacial to Holocene climate changes in the SE pacific. The Raraku lake sedimentary record (Easter Island, 27°S). Quat. Sci. Rev. 28, 2743–2759. https://doi.org/10.1016/j.quascirev.2009.06.018.
Saraswati, P.K., Srinivasan, M.S., 2015. Micropaleontology: Principles and Applications. Springer, Cham, Switzerland.
Saros, J.E., Michel, T.J., Interlandi, S.J., Wolfe, A.P., 2005. Resource requirements of *Asterionella formosa* and *Fragilaria crotonensis* in oligotrophic alpine lakes: implications for recent phytoplankton community reorganizations. Can. J. Fish. Aquat. Sci. 62, 1681–1689. https://doi.org/10.1139/f05-077.
Seddon, A.W.R., Mackay, A.W., Baker, A.G., Birks, H.J.B., Breman, E., Buck, C.E., Ellis, E.C., Froyd, C.A., Gill, J.L., Gillson, L., Johnson, E.A., Jones, V.J., Juggins, S., Macias-Fauria, M., Mills, K., Morris, J.L., Nogués-Bravo, D., Punyasena, S.W., Roland, T.P., Tanentzap, A.J., Willis, K.J., Aberhan, M., van Asperen, E.N., Austin, W.E.N., Battarbee, R.W., Bhagwat, S., Belanger, C.L., Bennett, K.D., Birks, H.H., Ramsey, C.B., Brooks, S.J., de Bruyn, M., Butler, P.G., Chambers, F.M., Clarke, S.J., Davies, A.L., Dearing, J.A., Ezard, T.H.G., Feurdean, A., Flower, R.J., Gell, P., Hausmann, S., Hogan, E.J., Hopkins, M.J., Jeffers, E.S., Korhola, A.A., Marchant, R., Kiefer, T., Lamentowicz, M., Larocque-Tobler, I., López-Merino, L., Liow, L.H., McGowan, S., Miller, J.H., Montoya, E., Morton, O., Nogué, S., Onoufriou, C., Boush, L.P., Rodríguez-Sánchez, F., Rose, N.L., Sayer, C.D., Shaw, H.E., Payne, R., Simpson, G., Sohar, K., Whitehouse, N.J., Williams, J.W., Witkowski, A., 2014. Looking forward through the past: identification of 50 priority research questions in palaeoecology. J. Ecol. 102, 256–267. https://doi.org/10.1111/1365-2745.12195.
Shotton, F.W., Williams, R.E.G., 1971. Birmingham university radiocarbon dates V. Radiocarbon 13, 141–156. https://doi.org/10.1017/S0033822200008419.
Sivarajah, B., Rühland, K.M., Labaj, A.L., Paterson, A.M., Smol, J.P., 2016. Why is the relative abundance of *Asterionella formosa* increasing in a Boreal Shield lake as nutrient levels decline? J. Paleolimnol. 55, 357–367. https://doi.org/10.1007/s10933-016-9886-2.
Skov, T., Buchaca, T., Amsinck, S.L., Landkildehus, F., Odgaard, B.V., Azevedo, J., Gonçalves, V., Raposeiro, P.M., Andersen, T.J., Jeppesen, E., 2010. Using invertebrate remains and pigments in the sediment to infer changes in trophic structure after fish introduction in Lake Fogo: a crater lake in the Azores. Hydrobiologia 654, 13–25. https://doi.org/10.1007/s10750-010-0325-5.
Šmilauer, P., Leps, J., 2014. Multivariate Analysis of Ecological Data Using CANOCO 5. Cambridge University Press, Cambridge, UK.
Sorvari, S., Korhola, A., Thompson, R., 2002. Lake diatom response to recent Arctic warming in Finnish Lapland. Global Change Biol. 8, 171–181. https://doi.org/10.1046/j.1365-2486.2002.00463.x.
Stone, J.R., Fritz, S.C., 2004. Three-dimensional modeling of lacustrine diatom habitat areas: improving paleolimnological interpretation of planktic : benthic ratios. Limnol. Oceanogr. 49, 1540–1548.
Stuiver, M., 1993. Editorial comment. Radiocarbon 35, iii. https://doi.org/10.1017/S0033822200013771.
Supico, F., 1995. As Escavações. Instituto Cultural de Ponta Delgada, Ponta Delgada, Portugal.
Talbot, M.R., 2001. Nitrogen isotopes in paleolimnology. In: Smol, J.P., Birks, H.J.B., Last, W.M. (Eds.), Tracking Environmental Change Using Lake Sediments. Volume 2: Physical and Geochemical Methods. Kluwer Academic Publishers, Dordrecht, Netherlands, pp. 401–439.
Telford, R.J., Barker, P., Metcalfe, S.E., Newton, A., 2004. Lacustrine responses to tephra deposition: examples from Mexico. Quat. Sci. Rev. 23, 2337–2353.
Ter Braak, C.J.F., Smilauer, P., 1998. CANOCO Reference Manual and User's Guide to CANOCO for Windows: Software for Canonical Community Ordination (Version 4). Microcomputer Power, Ithaca, NY.
Teranes, J.L., Bernasconi, S.M., 2005. Factors controlling $\delta^{13}C$ values of sedimentary carbon in hypertrophic Baldeggersee, Switzerland, and implications for interpreting isotope excursions in lake sedimentary records. Limnol. Oceanogr. 50, 914–922. https://doi.org/10.4319/lo.2005.50.3.0914.
Tilman, D., Kiesling, R., Sterner, R., Kilham, S., Johnson, F., 1986. Green, bluegreen and diatom algae: taxonomic differences in competitive ability for phosphorus, silicon and nitrogen. Arch. Hydrobiol. 106, 473–485.
Tilman, D., Kilham, S.S., Kilham, P., 1982. Phytoplankton community ecology: the role of limiting nutrients. Annu. Rev. Ecol. Systemat. 13, 349–372. https://doi.org/10.1146/annurev.es.13.110182.002025.
Vázquez-Loureiro, D., Gonçalves, V., Sáez, A., Hernández, A., Raposeiro, P.M., Giralt, S., Rubio-Inglés, M.J., Rull, V., Bao, R., 2019. Diatom-inferred ecological responses of an oceanic lake system to volcanism and anthropogenic perturbations since 1290 CE. Palaeogeogr. Palaeoclimatol. Palaeoecol. 534, 109285. https://doi.org/10.1016/j.palaeo.2019.109285.
Volkov, D.L., Fu, L.-L., 2010. On the reasons for the formation and variability of the Azores current. J. Phys. Oceanogr. 40, 2197–2220. https://doi.org/10.1175/2010JPO4326.1.
Wetzel, R.G., 2001. Limnology. Academic Press, San Diego, CA.
Williamson, C.E., Dodds, W., Kratz, T.K., Palmer, M.A., 2008. Lakes and streams as sentinels of environmental change in terrestrial and atmospheric processes. Front. Ecol. Environ. 6, 247–254. https://doi.org/10.1890/070140.
Williamson, C.E., Saros, J.E., Schindler, D.W., 2009. Sentinels of change. Science 323, 887–888. https://doi.org/10.1126/science.1169443.
Wolfe, A.P., Cooke, C.A., Hobbs, W.O., 2006. Are current rates of atmospheric nitrogen deposition influencing lakes in the Eastern Canadian Arctic? Arctic Antarct. Alpine Res. 38, 465–476. https://doi.org/10.1657/1523-0430(2006)38[465:ACROAN]2.0.CO;2.
Wolfe, A.P., Hobbs, W.O., Birks, H.H., Briner, J.P., Holmgren, S.U., Ingólfsson, Ó., Kaushal, S.S., Miller, G.H., Pagani, M., Saros, J.E., Vinebrooke, R.D., 2013. Stratigraphic expressions of the Holocene–Anthropocene transition revealed in sediments from remote lakes. Earth Sci. Rev. 116, 17–34. https://doi.org/10.1016/j.earscirev.2012.11.001.
Yamamoto, A., Palter, J.B., 2016. The absence of an Atlantic imprint on the multidecadal variability of wintertime European temperature. Nat. Commun. 7, 10930. https://doi.org/10.1038/ncomms10930.
Yu, Q., Liu, Z., Chen, Y., Zhu, D., Li, N., 2018. Modelling the impact of hydrodynamic turbulence on the competition between *Microcystis* and *Chlorella* for light. Ecol. Model. 370, 50–58. https://doi.org/10.1016/j.ecolmodel.2018.01.004.